

# Automated Security Response through Online Learning with Adaptive Conjectures

Kim Hammar<sup>†</sup>, Tao Li<sup>‡</sup>, Rolf Stadler<sup>†</sup>, and Quanyan Zhu<sup>‡</sup>

<sup>†</sup> Division of Network and Systems Engineering, KTH Royal Institute of Technology, Sweden

<sup>‡</sup> Department of Electrical and Computer Engineering, New York University, USA

Email: {kimham, stadler}@kth.se, {tl2636, qz494}@nyu.edu

February 21, 2024

arXiv:2402.12499v1 [cs.GT] 19 Feb 2024

**Abstract**—We study automated security response for an IT infrastructure and formulate the interaction between an attacker and a defender as a partially observed, non-stationary game. We relax the standard assumption that the game model is correctly specified and consider that each player has a probabilistic conjecture about the model, which may be misspecified in the sense that the true model has probability 0. This formulation allows us to capture uncertainty about the infrastructure and the intents of the players. To learn effective game strategies online, we design a novel method where a player iteratively adapts its conjecture using Bayesian learning and updates its strategy through rollout. We prove that the conjectures converge to best fits, and we provide a bound on the performance improvement that rollout enables with a conjectured model. To characterize the steady state of the game, we propose a variant of the Berk-Nash equilibrium. We present our method through an advanced persistent threat use case. Simulation studies based on testbed measurements show that our method produces effective security strategies that adapt to a changing environment. We also find that our method enables faster convergence than current reinforcement learning techniques.

**Index Terms**—Cybersecurity, network security, advanced persistent threat, APT, game theory, Bayesian learning, rollout.

## I. INTRODUCTION

An organization’s security strategy has traditionally been defined and updated by domain experts. Though this approach can provide basic security for an organization’s IT infrastructure, a growing concern is that infrastructure update cycles become shorter and attacks increase in sophistication. To address this challenge, game-theoretic methods for automating security strategies have been proposed, whereby the interaction between an attacker and a defender is modeled as a game [1]. While such methods can produce optimal security strategies, they rely on unrealistic assumptions about the infrastructure. In particular, most of the current methods are limited to stationary and correctly specified games, which assume a static infrastructure that can be accurately modeled without uncertainty [2]–[11]. These assumptions are unrealistic for several reasons.

First, IT infrastructures are *dynamic*: components fail, software packages are updated, new vulnerabilities are discovered, etc. As a consequence, the game between the attacker and the defender is *non-stationary*. Second, attacker and defender often have incorrect prior knowledge about the infrastructure and the opponent, which means that players generally have

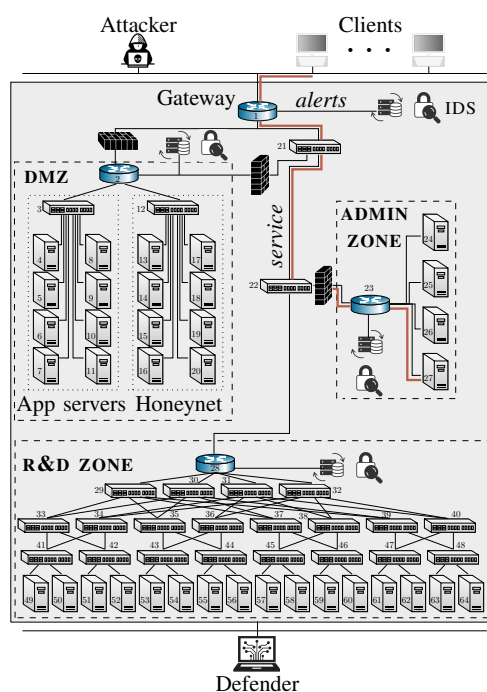


Fig. 1: The target infrastructure and the actors involved in the Advanced Persistent Threat (APT) use case.

*misspecified* models. Third, the defender has limited knowledge about an attacker’s presence and actions, which means that the game has *partial observability*.

In this paper, we address the above challenges and present a new game-theoretic method for *online learning* of security strategies that is applicable to dynamic IT environments where attacker and defender are uncertain about the environment and the opponent’s strategy. Using this method, we formulate the interaction between an attacker and a defender as a non-stationary, partially observed game. We relax the standard assumption that the game model is correctly specified and consider the case where each player has a probabilistic *conjecture* of the model, i.e., a probability distribution over possible models, which may be *misspecified* in the sense that the true model has probability 0. Both players iteratively adapt their conjecture using *Bayesian learning* and update their strategy using *rollout* [12]. We prove that the conjectures converge to best fits, and we provide a bound on the performance

improvement that rollout enables with a conjectured model. To characterize the steady state of the game, we define a variant of the *Berk-Nash equilibrium* [13, Def. 1], which represents a fixed point where players act optimally given their conjectures.

While the study of learning with misspecified models has attracted long-standing interest in economics [13], engineering [14], and psychology [15], it remains unexplored in the security context. Related research in the security literature include (i) game-theoretic approaches based on bounded rationality [11], [16]–[26]; and (ii) model-free learning techniques [4], [8], [9], [27]–[33]. (A review of related work can be found in §VIII.) To our knowledge, we provide the first study of learning with misspecified models in a security context. The benefit of this approach is threefold. First, it provides a new methodology to capture uncertainty and misspecification in security games. Second, as we show in this paper, it is applicable to dynamic, non-stationary, and partially observed games. Third, the model conjectures produced by our method are guaranteed to converge under reasonable conditions and the worst-case performance of the learned strategies is bounded.

We present our method through a use case that involves an Advanced Persistent Threat (APT) on an IT infrastructure (see Fig. 1). We emulate this infrastructure with a *digital twin*, on which we run APT actions and defender responses. During such runs, we collect measurements and logs, from which we estimate infrastructure statistics. This data is then used to instantiate simulations of the use case, based on which we evaluate our method. We find that the method produces effective security strategies that adapt to a changing environment. Simulation results further show that our method enables faster convergence than current reinforcement learning techniques.

### Contributions.

- 1) We introduce a novel game-theoretic formulation for the problem of automated security response where each player (i.e., attacker or defender) has a probabilistic conjecture about the game model. This formulation allows us to capture uncertainty about the environment and a player’s intent.
- 2) We present a new method for online learning of game strategies where a player iteratively adapts its conjecture using Bayesian learning and updates its strategy through rollout. This method allows us to automatically adapt security strategies to changes in the environment or the intent of the other player.
- 3) We prove that, when using our method, the conjectures of both players converge, and we characterize the steady state as a variant of the Berk-Nash equilibrium [13, Def. 1]. We also provide a bound on the performance improvement that rollout enables with a conjectured model.
- 4) We evaluate our method using simulation studies, which are based on measurements from a digital twin running 64 virtualized servers and 10 different types of APTs [34]. This evaluation provides insights into how our method performs under different conditions and shows that it outperforms current reinforcement learning techniques.

## II. USE CASE: ADVANCED PERSISTENT THREATS (APTS)

We consider the problem of defending the IT infrastructure of an organization against APTs. The operator of the infrastructure, which we call the *defender*, takes measures to protect it against an *attacker* while providing services to a client population (see Fig. 1). The infrastructure includes a set of servers and an Intrusion Detection System (IDS) that logs events in real-time. Clients access the services through a public gateway, which is also open to the attacker.

The attacker’s goal is to intrude on the infrastructure and compromise its servers. To achieve this goal, the attacker explores the infrastructure through reconnaissance and exploits vulnerabilities while trying to avoid detection.

The defender monitors the infrastructure through observing IDS alerts and other statistics. It can recover potentially compromised servers (e.g., by upgrading their software), which temporarily disrupts service for clients. When deciding to take this response action, the defender balances two conflicting objectives: (i) maintain services to its clients; and (ii) recover compromised servers.

### III. GAME MODEL OF THE APT USE CASE

We formulate the above use case as a zero-sum stochastic game with one-sided partial observability

$$\Gamma \triangleq \langle \mathcal{N}, \mathcal{S}, (\mathcal{A}_i)_{i \in \mathcal{N}}, f, c, \gamma, \mathbf{b}_1, \mathcal{O}, z \rangle, \quad (1)$$

where  $\mathcal{N}$  is the set of players,  $\mathcal{S}$  is the set of states,  $(\mathcal{A}_i)_{i \in \mathcal{N}}$  are the sets of actions, and  $\mathcal{O}$  is the set of observations;  $f$  is the transition function,  $c$  is the cost function, and  $z$  is the observation function;  $\gamma$  is the discount factor; and  $\mathbf{b}_1$  is the initial state distribution [35, Def. 3.1].  $\Gamma$  is a discrete-time game with two players: the (D)efender and the (A)ttacker.

The attacker and the defender have different observability in the game. The defender observes IDS alerts but has no certainty about the presence of an attacker. The attacker, on the other hand, has complete observability. It has access to all the information that the defender has access to, as well as the defender’s past actions. We can motivate this assumption in several ways. First, the assumption holds for many types of insider attacks [8]. Second, it reflects the fact that it is generally not known what information is available to the attacker [35]. Third, it significantly reduces the computational complexity of solving the game [36], [37].

In the following subsections, we define the components of the game, its evolution, and the objectives of the players.

**Notations.** Boldface lower case letters (e.g.,  $\mathbf{x}$ ) denote column vectors; upper case calligraphy letters (e.g.,  $\mathcal{V}$ ) represent sets. The set of probability distributions over  $\mathcal{V}$  is written as  $\Delta(\mathcal{V})$ .  $\mathbb{1}_{\mathcal{V}}(x)$  is the indicator function.  $\delta_{i,j}$  is Kronecker’s delta.  $\delta_i(\cdot)$  is the Dirac delta function. A random variable is written in upper case (e.g.,  $X$ ), a random vector in boldface (e.g.,  $\mathbf{X}$ ). The expectation of  $f$  with respect to  $X$  is written as  $\mathbb{E}_X[f]$ .  $x \sim f$  means that  $x$  is sampled from  $f$ . If the expression  $f$  includes many random variables that depend on  $\pi$ , we simply write  $\mathbb{E}_\pi[f]$ . We use  $\mathbb{P}[x|y]$  as a shorthand for  $\mathbb{P}[X = x|Y = y]$  and  $-k$  as a shorthand for  $\mathcal{N} \setminus k$ . Further notations are listed in Table 1.

$$\mathbb{B}(\mathbf{b}_{t-1}, a_{t-1}^{(D)}, o_t, \pi_A)(s_t) \triangleq \frac{z(o_t | s_t) \sum_{s_{t-1} \in \mathcal{S}} \sum_{a_{t-1}^{(A)} \in \mathcal{A}_A} \pi_A(a_{t-1}^{(A)} | \mathbf{b}_{t-1}, s_{t-1}) \mathbf{b}_{t-1}(s_{t-1}) f(s_t | s_{t-1}, a_{t-1}^{(D)}, a_{t-1}^{(A)})}{\sum_{a_{t-1}^{(A)} \in \mathcal{A}_A} \sum_{s', s \in \mathcal{S}} z(o_t | s') \pi_A(a_{t-1}^{(A)} | s, \mathbf{b}_{t-1}) f(s' | s, a_{t-1}^{(D)}, a_{t-1}^{(A)}) \mathbf{b}_{t-1}(s)}. \quad (6)$$

Notation(s)	Description
$\Gamma, c, N$	The game (1), cost function (7), and # servers (§III-B)
$D, A$	The defender player and the attacker player (1)
$\mathcal{N}, \mathcal{S}, \mathcal{O}$	Sets of players, states, and observations (1)
$\mathcal{A}_D, \mathcal{A}_A$	Sets of defender and attacker actions (1)
$t, \gamma$	Time step and discount factor (8)
$\pi_D, \pi_A$	Defender and attacker strategies (§III-D)
$\Pi = \Pi_D \times \Pi_A$	Defender and attacker strategy spaces (§III-D)
$\tilde{\pi}_D, \tilde{\pi}_A$	Best response strategies (9)
$\pi^* = (\pi_D^*, \pi_A^*)$	Optimal strategies (11)
$\mathcal{B}_D, \mathcal{B}_A$	Best response correspondences (9)
$J_D, J_A$	Defender and attacker objectives (8)
$f, z$	Transition function (2) and observation function (4)
$s_t, o_t$	State (2) and observation (4) at time $t$
$\mathbf{a}_t = (a_t^{(D)}, a_t^{(A)})$	Actions at time $t$ (§III-A)
$S_t, O_t$	Random variables with realizations $s_t$ (2) and $o_t$ (4)
$\mathbf{A}_t$	Random vector with realization $\mathbf{a}_t$ (§III-A)
$\mathbf{b}_t, \mathbf{B}_t$	Defender belief ( $\mathbf{b}_t$ realizes the random vector $\mathbf{B}_t$ ) (5)
$\mathcal{B}, \mathbb{B}$	Belief space and belief operator of the defender (6)
$\mathbf{h}_t^{(k)}, \mathbf{h}_t$	History of player $k$ and joint history (§III-C)
$\mathbf{H}_t^{(k)}, \mathbf{H}_t$	Random vectors with realizations $\mathbf{h}_t^{(k)}$ and $\mathbf{h}_t$ (§III-C)
$\mathcal{H} = \mathcal{H}_D \times \mathcal{H}_A$	History spaces (§III-C)
$S, C$	Stop and continue actions (§III-A)
$\mathcal{R}$	Rollout operator for online learning (13)
$\bar{\pi}_{-k,t}$	Player $k$ 's conjecture of player $-k$ 's strategy (Alg. 1)
$\bar{\ell}_D, \bar{\ell}_A$	Lookahead horizons (Alg. 1)
$\bar{\ell}_{-k,t}$	Player $k$ 's conjecture of player $-k$ 's lookahead (Alg. 1)
$\boldsymbol{\theta}_t$	Parameter vector of $\Gamma$ at time $t$ (16a)
$\bar{\boldsymbol{\theta}}_t^{(k)}$	Player $k$ 's conjecture of $\boldsymbol{\theta}_t$ at time $t$ (16a)
$\mathcal{L}, \Theta_k$	Player $k$ 's sets of possible conjectures of $\ell_A$ and $\boldsymbol{\theta}$ (16)
$\mathcal{L}^*, \Theta_k^*$	Sets of consistent conjectures (18)
$\mathbf{i}_t^{(k)}, \mathbf{I}_t^{(k)}$	Information feedback of player $k$ at time $t$ (3)
$\mu_t, \rho_t^{(k)}$	Posteriors $\mathbb{P}[\ell_A   \mathbf{h}_t^{(D)}]$ (16b) and $\mathbb{P}[\boldsymbol{\theta}_t^{(k)}   \mathbf{h}_t^{(k)}]$ (16a)
$\nu, K(\bar{\alpha}, \nu)$	Occupancy measure and discrepancy of conjecture $\bar{\alpha}$ (17)
$\pi_{1,k}, \pi_{t,k}$	Base and rollout strategy of player $k$ at time $t$ (13)
$\pi_{\mathbf{h}_t}$	Strategy profile induced by Alg. 1 at time $t$ (§V-A)
$\mathbb{P}^{\mathcal{R}}$	Distribution over $\mathcal{H}_D \times \mathcal{H}_A$ for $\pi_{\mathbf{h}_t}$ (Thm. 4)
$K_{\mathcal{L}}^*, K_{\Theta_k}^*$	Minimal discrepancy values for $\mathcal{L}$ and $\Theta_k$ (18)

TABLE 1: Notations.

### A. Actions

Both players can invoke two actions: (S)top and (C)ontinue. The action spaces are thus  $\mathcal{A}_D \triangleq \mathcal{A}_A \triangleq \{S, C\}$ . S triggers a change in the game state while C is a passive action that does not change the state. Specifically,  $a_t^{(A)} = S$  is the attacker's compromise action and  $a_t^{(D)} = S$  is the defender's recovery action (as defined in the use case §II).

### B. Dynamics

The state  $s_t \in \mathcal{S} \triangleq \{0, 1, \dots, N\}$  represents the number of compromised servers at time  $t$ , where  $s_1 = 0$ . The transition  $s_t \rightarrow s_{t+1}$  occurs with probability  $f(s_{t+1} | s_t, a_t^{(D)}, a_t^{(A)})$ :

$$f(S_{t+1} = 0 | s_t, S, a_t^{(A)}) \triangleq 1 \quad (2a)$$

$$f(S_{t+1} = s_t | s_t, C, C) \triangleq 1 \quad (2b)$$

$$f(S_{t+1} = s_t | s_t, C, S) \triangleq 1 - p_A \quad (2c)$$

$$f(S_{t+1} = \min[s_t + 1, N] | s_t, C, S) \triangleq p_A, \quad (2d)$$

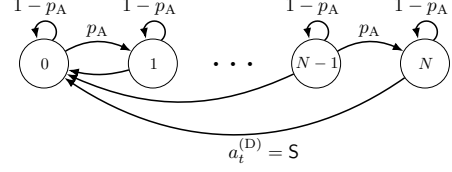


Fig. 2: State transition diagram of the game: disks represent states; arrows represent state transitions; labels indicate probabilities and conditions for state transition; the initial state is  $s_1 = 0$ .

where  $p_A$  is the probability of a successful attack. All other transitions have probability 0 (see Fig. 2).

(2a) defines the transition  $s_t \rightarrow 0$ , which occurs when the defender takes action S. (2b)–(2c) define the recurrent transition  $s_{t+1} = s_t$ , which occurs when both players take action C or when the attacker is unsuccessful in compromising a server, which happens with probability  $1 - p_A$ . Lastly, (2d) defines the transition  $s_t \rightarrow s_t + 1$ , which occurs with probability  $p_A$  when the attacker takes action S and the defender takes action C.

### C. Observability

The attacker has complete observability. It knows the game state, the defender's actions, and the defender's observations. In contrast, the defender has a finite set of observations  $o_t \in \mathcal{O}$ . Consequently, the *information feedbacks* for the attacker and the defender at time  $t$  are

$$\mathbf{i}_t^{(A)} \triangleq (o_t, s_t, a_{t-1}^{(D)}) \quad \text{and} \quad \mathbf{i}_t^{(D)} \triangleq (o_t), \quad (3)$$

respectively, where  $o_t$  is drawn from a random variable  $O_t$  whose distribution depends on the state, i.e.,

$$o_t \sim z(\cdot | s_t). \quad (4)$$

Both players  $k$  have *perfect recall*, which means that they remember the play history  $\mathbf{h}_t^{(k)} \triangleq (\mathbf{b}_1, a_1^{(k)}, \mathbf{i}_1^{(k)})_{l=1,2,\dots} \in \mathcal{H}_k$ . Based on this history, the defender computes the *belief state*  $\mathbf{b}_t \in \mathcal{B}$ , which is defined as

$$\mathbf{b}_t(s_t) \triangleq \mathbb{P}[S_t = s_t | \mathbf{h}_t^{(D)}], \quad (5)$$

where  $\mathbf{b}_t$  is computed recursively through the operator  $\mathbb{B}$  (6), which is defined at the top of the page.

### D. Strategies and Objectives

Since  $\mathbf{b}_t$  is a sufficient statistic for the Markovian state  $s_t$  (2), we can define the players' *behavioral strategies* as  $\pi_D \in \Pi_D \triangleq \mathcal{B} \rightarrow \Delta(\mathcal{A}_D)$  and  $\pi_A \in \Pi_A \triangleq \mathcal{B} \times \mathcal{S} \rightarrow \Delta(\mathcal{A}_A)$ .

The performance of a defender strategy is quantified using the following cost function

$$c(s_t, a_t^{(D)}) \triangleq \overbrace{s_t^p (1 - \delta_{S, a_t^{(D)}})}^{\text{intrusion cost}} + \overbrace{\delta_{S, a_t^{(D)}} (q - r \operatorname{sgn}(s_t))}^{\text{response action cost}}, \quad (7)$$

where  $p$ ,  $q$ , and  $r$  are scalar constants (see Fig. 3).

The goal of the defender is to *minimize* the expected cumulative cost and the goal of the attacker is to *maximize* the same quantity. Therefore, the objective functions are

$$J_D^{(\pi_D, \pi_A)}(\mathbf{b}_1) \triangleq \mathbb{E}_{(\pi_D, \pi_A)} \left[ \sum_{t=1}^{\infty} \gamma^{t-1} c(S_t, A_t^{(D)}) \mid \mathbf{b}_1 \right] \quad (8a)$$

$$J_A^{(\pi_D, \pi_A)}(\mathbf{b}_1) \triangleq -J_D^{(\pi_D, \pi_A)}(\mathbf{b}_1), \quad (8b)$$

where  $\gamma \in [0, 1)$  is a discount factor and  $\mathbb{E}_{(\pi_D, \pi_A)}$  is the expectation over the random vectors  $(\mathbf{H}_t^{(D)}, \mathbf{H}_t^{(A)})_{t \in \{1, 2, \dots\}}$  when the game is played according to  $(\pi_D, \pi_A)$ .

A defender strategy  $\tilde{\pi}_D \in \Pi_D$  is a *best response* against  $\pi_A \in \Pi_A$  if it *minimizes*  $J_D^{(\pi_D, \pi_A)}$  (8a). Similarly, an attacker strategy  $\tilde{\pi}_A$  is a best response against  $\pi_D$  if it *maximizes*  $J_D^{(\pi_D, \pi_A)}$  (8b). Hence, the best response correspondences are

$$\mathcal{B}_D(\pi_A) \triangleq \arg \min_{\pi_D \in \Pi_D} J_D^{(\pi_D, \pi_A)}(\mathbf{b}_1) \quad (9a)$$

$$\mathcal{B}_A(\pi_D) \triangleq \arg \max_{\pi_A \in \Pi_A} J_D^{(\pi_D, \pi_A)}(\mathbf{b}_1). \quad (9b)$$

When the infrastructure contains a single server ( $N = 1$ ), there exist best responses with *threshold structure*, as stated below.

**Theorem 1.** *If  $N = 1$  and  $z$  (4) is totally positive of order 2 (i.e., TP-2 [38, Def. 10.2.1]), then*

(A) *For any  $\pi_A \in \Pi_A$ , there exists a value  $\alpha^* \in [0, 1]$  and a best response  $\tilde{\pi}_D \in \mathcal{B}_D(\pi_A)$  (9a) that satisfies*

$$\tilde{\pi}_D(b_t) = S \iff b_t \geq \alpha^*. \quad (10a)$$

(B) *For any  $\pi_D \in \Pi_D$  that satisfies (10a), there exists a value  $\beta^* \in [0, 1]$  and a best response  $\tilde{\pi}_A \in \mathcal{B}_A(\pi_D)$  (9b) that satisfies*

$$\tilde{\pi}_A(s_t, b_t) = S \iff s_t = 0, b_t < \beta^*. \quad (10b)$$

*Proof.* See Appendix A.  $\square$

The above theorem implies that, when  $N = 1$ , the best responses can be parameterized by thresholds, which allows to formulate (9a)–(9b) as parametric optimization problems. Figure 4 shows the convergence curves when performing these optimizations with the Cross-Entropy Method (CEM) [39].

### E. Equilibria

When the attacker and the defender play best response, their strategy pair is a *Nash equilibrium* and can be written as [40]

$$\boldsymbol{\pi}^* = (\pi_D^*, \pi_A^*) \in \mathcal{B}_D(\pi_A^*) \times \mathcal{B}_A(\pi_D^*). \quad (11)$$

This equilibrium solves the following minimax problem [41]

$$\underset{\pi_D \in \Pi_D}{\text{minimize}} \underset{\pi_A \in \Pi_A}{\text{maximize}} J_D^{(\pi_D, \pi_A)}(\mathbf{b}_1) \quad (12a)$$

$$\text{subject to } s_{t+1} \sim f(\cdot \mid s_t, \mathbf{a}_t) \quad \forall t \quad (12b)$$

$$o_{t+1} \sim z(\cdot \mid s_t) \quad \forall t \quad (12c)$$

$$a_t^{(A)} \sim \pi_A(\cdot \mid s_t, \mathbf{b}_t) \quad \forall t \quad (12d)$$

$$a_t^{(D)} \sim \pi_D(\cdot \mid \mathbf{b}_t) \quad \forall t \quad (12e)$$

$$s_1 \sim \mathbf{b}_1, \quad (12f)$$

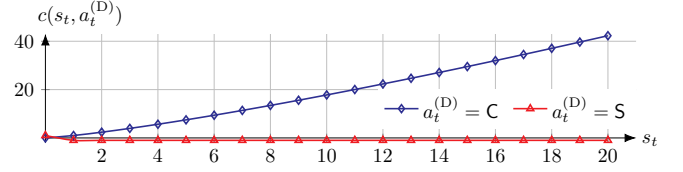


Fig. 3: An example cost function  $c(s_t, a_t^{(D)})$  (7) of  $\Gamma$  (1).

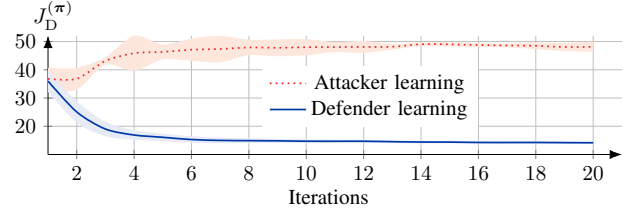


Fig. 4: Best response learning when  $N = 1$  using CEM [39] and the threshold parameterization expressed in Thm. 1; the curves show the mean and the 95% confidence interval from evaluations with 20 random seeds; hyperparameters are listed in Appendix F.

where (12b) is the dynamics constraint; (12c) describes the observations; (12d)–(12e) capture the actions; and (12f) defines the initial state distribution. (Remark: As a solution to (12) exists [37, Thm. 2.3], we write min max instead of inf sup.)

While any strategy pair  $\boldsymbol{\pi}^*$  that satisfies (11) is a Nash equilibrium, (12) implies that  $\boldsymbol{\pi}^*$  together with  $\mathbb{B}$  (6) form a stronger equilibrium, namely a *perfect Bayesian equilibrium* [42, Defs. 8.2-3][43].

**Definition 1** (Perfect Bayesian equilibrium).  $\boldsymbol{\pi}^*$  (11) and  $\mathbb{B}$  (6) is a *perfect Bayesian equilibrium* iff

1)  $\boldsymbol{\pi}^*$  is a Nash equilibrium in  $\Gamma|_{\mathbf{h}_t^{(D)}} \forall \mathbf{h}_t^{(D)} \in \mathcal{H}_D$ ,

where  $\Gamma|_{\mathbf{h}_t^{(D)}}$  is the subgame starting from  $\mathbb{B}(\mathbf{h}_t^{(D)}, \pi_A^*)$ .

2) For any  $\mathbf{h}_t^{(D)} \in \mathcal{H}_D$  with  $\mathbb{P}[\mathbf{h}_t^{(D)} \mid \boldsymbol{\pi}^*, \mathbf{b}_1] > 0$ , then

$$\mathbb{B}(\mathbf{h}_t^{(D)}, \pi_A^*) = \mathbb{B}(\mathbb{B}(\mathbf{h}_{t-1}^{(D)}, \pi_A^*), \pi_D^*(\mathbb{B}(\mathbf{h}_{t-1}^{(D)}, \pi_A^*), o_t, \pi_A^*)).$$

**Theorem 2.** *Given the instantiation of  $\Gamma$  described in §III, the following holds.*

(A)  $|\mathcal{B}_D(\pi_A)| > 0$  and  $|\mathcal{B}_A(\pi_D)| > 0 \forall (\pi_A, \pi_D)$ .

(B)  $\Gamma$  has a *perfect Bayesian equilibrium* (Def. 1).

*Proof.* Since  $\Gamma$  is finite and  $\gamma \in [0, 1)$ , (A) follows from [38, Thms. 7.6.1-7.6.2][44, Thm. 6, p. 160]. We omit the proof as it is standard in Markov decision theory. Readers familiar with the literature are encouraged to consult [38] for the details. We prove (B) by construction. For any *reachable* subgame, a Nash equilibrium  $\boldsymbol{\pi}^*$  exists [45, §3][37, Thm. 2.3]. For any *unreachable* subgame  $\Gamma|_{\mathbf{h}_k^{(D)}}$ , we can construct another Nash equilibrium  $\boldsymbol{\pi}^{*,k}$ . This follows because the proofs in [45, §3][37, Thm. 2.3] do not depend on  $\mathbf{b}_1$ . By combining  $\boldsymbol{\pi}^*$  with the equilibria of all unreachable subgames, we obtain a perfect Bayesian equilibrium (Def. 1).  $\square$

Figure 5 shows the value of a perfect Bayesian equilibrium (Def. 1) when  $N = 1$ . Interestingly, the defender has the highest expected cost when the belief of compromise  $(\mathbf{b}(1))$  is around 0.35 rather than 0.5.

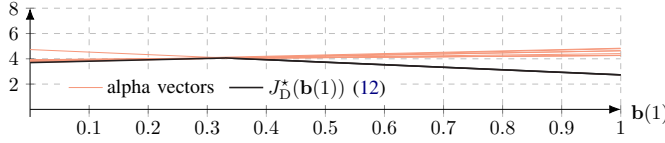


Fig. 5: The equilibrium value (12) of  $\Gamma$  when  $N = 1$  (computed with the HSVI algorithm [46, Alg. 1]); hyperparameters are listed in Appendix F.

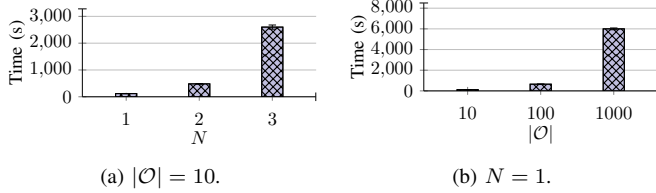


Fig. 6: Time required to compute a perfect Bayesian equilibrium (Def. 1) of  $\Gamma$  (1) with HSVI [46, Alg. 1] for different values of  $N$  (Fig. 6a) and  $|\mathcal{O}|$  (Fig. 6b); error bars indicate the 95% confidence interval based on 20 measurements; hyperparameters are listed in Appendix F.

#### IV. PROBLEM STATEMENT

While the equilibrium defined above describes how the game *ought to be played* by rational players, computing it is intractable for any realistic instantiation of the game, as illustrated in Fig. 6. Further, the equilibrium assumes a stationary game where both players have correctly specified models, which is not the case in practice. To address these limitations, we relax the standard assumptions and consider a setting where the game is *non-stationary* and where players may have *misspecified* game models. In particular, we consider the following problem.

**Problem 1** (Non-stationary game with misspecification). We consider a game  $\Gamma_{\theta_t}$  based on (1) that is parameterized by a time-dependent vector  $\theta_t$ , which is hidden from the players. This vector can represent the transition function (2), the observation function (4), etc. Player  $k$  has a *conjecture* of  $\theta_t$ , denoted by  $\bar{\theta}_t^{(k)} \in \Theta_k$ , which is *misspecified* if  $\theta_t \notin \Theta_k$ . As  $\theta_t$  evolves, player  $k$  adapts its conjecture based on feedback  $\mathbf{i}_t^{(k)}$  (3) and uses the conjecture to update its strategy  $\pi_{k,t}$ , starting from a *base strategy*  $\pi_{k,1}$ . Strategy updates are parameterized by a *lookahead horizon*  $\ell_k$ , which can be understood as a computational constraint. The defender conjectures  $\ell_A$  as  $\bar{\ell}_A \in \mathcal{L}$ , which captures the defender’s uncertainty about the attacker’s intent. We assume that the attacker knows  $\ell_D$  and the defender’s conjectures.

Solving the game described in Prob. 1 leads to the following questions.

- (i) What is an effective method for a player to update its conjecture and its strategy?
- (ii) Do the sequences of conjectures converge?
- (iii) Once the parameters  $\theta_t$  remain constant, how can the steady state of  $\Gamma_{\theta_t}$  be characterized?

#### V. ONLINE LEARNING WITH ADAPTIVE CONJECTURES

We address the above questions and define a game-theoretic method for *online learning* in  $\Gamma_{\theta_t}$  (Prob. 1). Using our method,

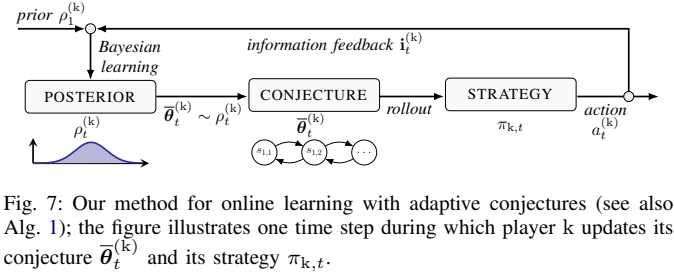


Fig. 7: Our method for online learning with adaptive conjectures (see also Alg. 1); the figure illustrates one time step during which player  $k$  updates its conjecture  $\bar{\theta}_t^{(k)}$  and its strategy  $\pi_{k,t}$ .

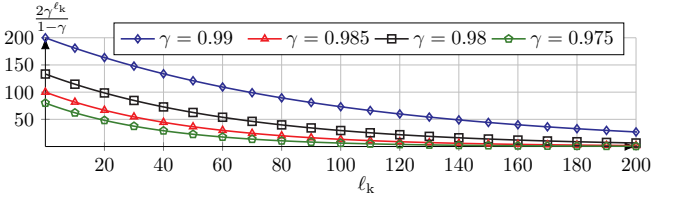


Fig. 8: Illustration of Thm. 3; the x-axis indicates the lookahead horizon  $\ell_k$ ; the y-axis indicates the factor of the performance bound in (15b); the curves relate to different discount factors  $\gamma$ .

each player iteratively adapts its conjecture through *Bayesian learning* and updates its strategy through *rollout* (see Fig. 7). The pseudocode of our method is listed in Alg. 1. The main steps of the algorithm are described below.

At time  $t$ , player  $k$  updates its base strategy  $\pi_{k,1}$  as follows.

$$\pi_{k,t}(\mathbf{b}_t) \in \mathcal{R}(\bar{\theta}_t^{(k)}, \mathbf{b}_t, \bar{J}_k^{(\pi_t)}, \ell_k) \triangleq \arg \min_{a_t^{(k)}, a_{t+1}^{(k)}, \dots, a_{t+\ell_k-1}^{(k)}} \mathbb{E}_{\pi_t} \left[ \sum_{j=t}^{t+\ell_k-1} \gamma^{j-t} c_k(S_j, A_j^{(D)}) + \gamma^{\ell_k} \bar{J}_k^{(\pi_t)}(\mathbf{B}_{t+\ell_k}) \mid \mathbf{b}_t \right], \quad (13)$$

where  $\ell_k$  is the lookahead horizon,  $c_D = c$  (7),  $c_A = -c$ , and  $\bar{J}_k^{(\pi_t)}$  is the cost function induced by  $\bar{\theta}_t^{(k)}$  (line 19 in Alg. 1).

This rollout step depends on the strategy of the opponent, i.e.,  $\pi_t = (\pi_{k,1}, \pi_{-k,t})$ . Since the base strategies  $(\pi_{A,1}, \pi_{D,1})$  are known to both players, each player can obtain a conjecture of the opponent’s strategy from  $\bar{\ell}_{-k}$  (lines 14–17 in Alg. 1).

We know from dynamic programming that  $\pi_{k,t}$  (13) improves on the base strategy  $\pi_{k,1}$  [47, Prop. 1]. The extent of the improvement depends on the lookahead horizon and the accuracy of the conjectures as follows.

**Theorem 3.** *The conjectured cost of player  $k$ ’s rollout strategy  $\pi_{k,t}$  satisfies*

$$\bar{J}_k^{(\pi_{k,t}, \bar{\pi}_{-k,t})}(\mathbf{b}) \leq \bar{J}_k^{(\pi_{k,1}, \bar{\pi}_{-k,t})}(\mathbf{b}) \quad \forall \mathbf{b} \in \mathcal{B}. \quad (15a)$$

Assuming  $(\bar{\theta}_t^{(k)}, \bar{\ell}_{-k})$  predicts the game  $\ell_k$  steps ahead, then

$$\|\bar{J}_k^{(\pi_{k,t}, \bar{\pi}_{-k,t})} - J_k^*\| \leq \frac{2\gamma^{\ell_k}}{1-\gamma} \|\bar{J}_k^{(\pi_{k,1}, \bar{\pi}_{-k,t})} - J_k^*\|, \quad (15b)$$

where  $J_k^*$  is the optimal cost-to-go function when facing  $\pi_{-k,t}$ .  $\|\cdot\|$  is the maximum norm  $\|J\| = \max_x |J(x)|$ .

*Proof.* See Appendix B.  $\square$

Theorem 3 states that the performance bound improves superlinearly when the lookahead horizon  $\ell_k$  increases or when the conjectured cost function  $\bar{J}_k$  moves closer to  $J_k^*$

(9), as shown in Fig. 8. In particular, (15b) suggests that  $\ell_k$  controls the trade-off between computational cost and rollout performance (see Fig. 9).

After computing (13) and executing the corresponding action, player k receives the feedback  $\mathbf{i}_t^{(k)}$  (3) and updates its conjectures as  $\bar{\theta}_t^{(k)} \sim \rho_t^{(k)}$  and  $\bar{\ell}_{A,t} \sim \mu_t$  (line 14 in Alg. 1), where  $\rho_t^{(k)}$  and  $\mu_t$  are adapted through *Bayesian learning* as

$$\rho_t^{(k)}(\bar{\theta}_t^{(k)}) \triangleq \frac{\mathbb{P}[\mathbf{i}_t^{(k)} | \bar{\theta}_t^{(k)}, \mathbf{b}_{t-1}] \rho_{t-1}^{(k)}(\bar{\theta}_{t-1}^{(k)})}{\int_{\Theta_k} \mathbb{P}[\mathbf{i}_t^{(k)} | \bar{\theta}_t^{(k)}, \mathbf{b}_{t-1}] \rho_{t-1}^{(k)}(d\bar{\theta}_t^{(k)})} \quad (16a)$$

$$\mu_t(\bar{\ell}_A) \triangleq \frac{\mathbb{P}[\mathbf{i}_t^{(D)} | \bar{\ell}_A, \mathbf{b}_{t-1}] \mu_{t-1}(\bar{\ell}_A)}{\sum_{\bar{\ell}_A \in \mathcal{L}} \mathbb{P}[\mathbf{i}_t^{(D)} | \bar{\ell}_A, \mathbf{b}_{t-1}] \mu_{t-1}(\bar{\ell}_A)}. \quad (16b)$$

These Bayesian updates are well-defined using the following assumption.

**Assumption 1.** (i)  $\mathcal{L}$  is finite and  $\Theta_k$  is a compact subset of an Euclidean space; (ii)  $\rho_1^{(k)}$  and  $\mu_1$  have full support; and (iii) for all feasible  $(\mathbf{i}^{(k)}, \mathbf{b}_t)$ , there exists  $\bar{\theta} \in \Theta_k$  and  $\bar{\ell}_A \in \mathcal{L}$  that assign positive probability to  $\mathbf{i}^{(k)}$  in  $\mathbf{b}_t$ .

**Algorithm 1:** Online learning with adaptive conjectures.

```

1 Input: Initial belief  $\mathbf{b}_1$ , game model  $\Gamma_{\theta_1}$ ,
2 base strategies  $\pi_1 \triangleq (\pi_{D,1}, \pi_{A,1})$ , priors  $(\mu_1, \rho_1^{(D)}, \rho_1^{(A)})$ ,
3 discount factor  $\gamma$ , lookahead horizons  $\ell_D, \ell_A$ .
4 Output: A sequence of action profiles  $\mathbf{a}_1, \mathbf{a}_2, \dots$ 
5 Algorithm
6   /* Initialization */
7    $\mathbf{h}_1^{(D)} \leftarrow (\mathbf{b}_1), \mathbf{h}_1^{(A)} \leftarrow (\mathbf{b}_1)$ ,
8    $s_1 \sim \mathbf{b}_1$ 
9    $\bar{\pi}_{A,1} \leftarrow \pi_{A,1}, \bar{\pi}_{D,1} \leftarrow \pi_{D,1}$ 
10   $\mathbf{a}_1^{(D)} \sim \pi_{D,1}(\mathbf{b}_1), \mathbf{a}_1^{(A)} \sim \pi_{A,1}(\mathbf{b}_1, s_1)$ 
11   $s_2 \sim f(\cdot | s_1, (\mathbf{a}_1^{(D)}, \mathbf{a}_1^{(A)}))$ 
12  for  $t = 2, 3, \dots$  do
13    /* Defender learning */
14     $o_t \sim z(\cdot | s_t)$ 
15     $\mathbf{i}_t^{(D)} \leftarrow (o_t), \mathbf{h}_t^{(D)} \leftarrow (\mathbf{h}_{t-1}^{(D)}, \mathbf{i}_t^{(D)}, a_{t-1}^{(D)})$ 
16    Update  $\rho_t^{(D)}$  and  $\mu_t$  (16) and set  $\bar{\theta}_t^{(D)} \sim \rho_t^{(D)}$  and  $\bar{\ell}_{A,t} \sim \mu_t$ 
17     $\mathbf{b}_t \leftarrow \mathbb{E}(\mathbf{h}_t^{(D)}, \bar{\pi}_{A,t-1})$ 
18    Estimate  $\bar{J}_A^{(\pi_{D,t-1}, \pi_{A,1})}$  using  $\Gamma_{\bar{\theta}_t^{(D)}}$ 
19    Compute  $\bar{\pi}_{A,t}(\mathbf{b}_t) \in \mathcal{R}(\bar{\theta}_t^{(D)}, \mathbf{b}_t, \bar{J}_A^{(\pi_{D,t-1}, \pi_{A,1})}, \bar{\ell}_{A,t})$ 
20    Estimate  $\bar{J}_D^{(\pi_{D,t-1}, \bar{\pi}_{A,t})}$  using  $\Gamma_{\bar{\theta}_t^{(D)}}$ 
21     $\pi_{D,t}(\mathbf{b}_t) \in \mathcal{R}(\bar{\theta}_t^{(D)}, \mathbf{b}_t, \bar{J}_D^{(\pi_{D,t-1}, \bar{\pi}_{A,t})}, \ell_D)$ 
22    /* Attacker learning */
23     $\mathbf{i}_t^{(A)} \leftarrow (o_t, s_t, a_{t-1}^{(D)}), \mathbf{h}_t^{(A)} \leftarrow (\mathbf{h}_{t-1}^{(A)}, \mathbf{i}_t^{(A)}, a_{t-1}^{(A)})$ 
24    Update  $\rho_t^{(A)}$  using (16a) and set  $\bar{\theta}_t^{(A)} \sim \rho_t^{(A)}$ 
25    Estimate  $\bar{J}_A^{(\pi_{A,1}, \pi_{D,t})}$  using  $\Gamma_{\bar{\theta}_t^{(A)}}$ 
26     $\pi_{A,t}(\mathbf{b}_t) \in \mathcal{R}(\bar{\theta}_t^{(A)}, \mathbf{b}_t, \bar{J}_A^{(\pi_{A,1}, \pi_{D,t})}, \ell_A)$ 
27     $\mathbf{a}_t^{(D)} \sim \pi_{D,t}(\mathbf{b}_t), \mathbf{a}_t^{(A)} \sim \pi_{A,t}(\mathbf{b}_t, s_t)$ 
28     $s_{t+1} \sim f(\cdot | s_t, (\mathbf{a}_t^{(D)}, \mathbf{a}_t^{(A)}))$ 
29  end

```

### A. Convergence and Equilibrium Analysis

When player k updates its conjectures through (16), the goal is to minimize the *discrepancy* between the feedback distributions induced by the conjectures and the true model (3). We define this discrepancy as

$$K(\bar{\alpha}, \nu) \triangleq \mathbb{E}_{\mathbf{b} \sim \nu} \mathbb{E}_{\mathbf{I}^{(k)}} \left[ \ln \left( \frac{\mathbb{P}[\mathbf{I}^{(k)} | \alpha, \mathbf{b}]}{\mathbb{P}[\mathbf{I}^{(k)} | \bar{\alpha}, \mathbf{b}]} \right) | \alpha, \mathbf{b} \right], \quad (17)$$

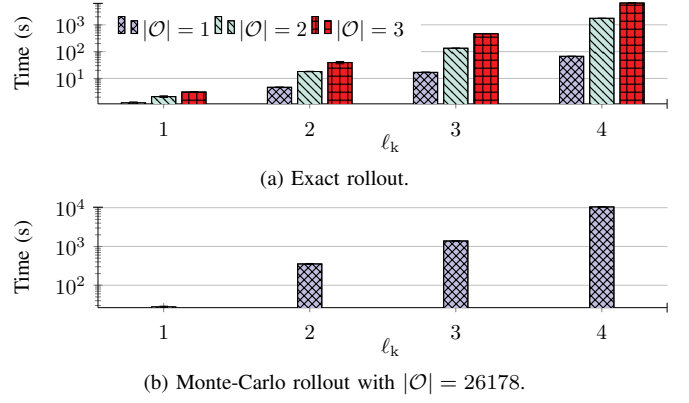


Fig. 9: Compute time of the rollout operator (13) for varying lookahead horizons  $\ell_k$  and observation space sizes  $|\mathcal{O}|$ ; hyperparameters are listed in Appendix F.

where  $\alpha \in \{\theta, \ell_A\}$  and  $\nu \in \Delta(\mathcal{B})$  is an occupancy measure. We say that conjectures that minimize (17) are *consistent* with  $\nu$  [48]<sup>1</sup>. Hence, the sets of consistent conjectures at time  $t$  are

$$\bar{\theta}_t^{(k)} \in \Theta_k^*(\nu_t) \triangleq \arg \min_{\bar{\theta}_t^{(k)} \in \Theta_k} K(\bar{\theta}_t^{(k)}, \nu_t) \quad (18a)$$

$$\bar{\ell}_{A,t} \in \mathcal{L}^*(\nu_t) \triangleq \arg \min_{\bar{\ell}_{A,t} \in \mathcal{L}} K(\bar{\ell}_{A,t}, \nu_t), \quad (18b)$$

where  $\nu_t \triangleq \frac{1}{t} \sum_{\tau=1}^t \mathbb{1}_{\{\mathbf{b}\}}(\mathbf{b}_\tau)$  is the empirical occupancy measure and  $\pi_{\mathbf{h}_t}$  is the empirical strategy profile induced by Alg. 1 at time  $t$ .

Intuitively,  $\Theta_k^*$  and  $\mathcal{L}^*$  contain the conjectures that player k considers possible after observing feedback generated by  $\nu_t$  and  $\pi_{\mathbf{h}_t}$  [49]. A desirable property of the conjecture distributions (16) is, therefore, that they concentrate on  $\Theta_k^*$  and  $\mathcal{L}^*$  (18). This property is guaranteed asymptotically under the following conditions.

**Assumption 2** (Regularity conditions). *For fixed values of  $\mathbf{i}^{(k)}$  and  $\theta$ ,*

- 1) *The mapping  $\mathbf{b} \mapsto \ln \mathbb{P}[\mathbf{i}^{(k)} | \theta, \mathbf{b}]$  is Lipschitz w.r.t. the Wasserstein-1 distance, and the Lipschitz constant is independent of  $\mathbf{i}^{(k)}$  and  $\theta$ .*
- 2) *The mapping  $\theta \mapsto \ln \mathbb{P}[\mathbf{i}^{(k)} | \theta, \mathbf{b}]$  is continuous and there exists an integrable function  $g_{\mathbf{b}}(\mathbf{i}^{(k)})$  for all  $\mathbf{b} \in \mathcal{B}$  such that  $|\ln \frac{\mathbb{P}[\mathbf{i}^{(k)} | \theta, \mathbf{b}]}{\mathbb{P}[\mathbf{i}^{(k)} | \bar{\theta}, \mathbf{b}]}| \leq g_{\mathbf{b}}(\mathbf{i}^{(k)})$  for all  $\bar{\theta} \in \Theta_k$ .*

**Theorem 4.** *Given Assumptions 1–2, the following holds for any sequence  $(\pi_{\mathbf{h}_t}, \nu_t)_{t \geq 1}$  generated by Alg. 1*

$$\lim_{t \rightarrow \infty} \sum_{\bar{\ell}_A \in \mathcal{L}} (K(\bar{\ell}_A, \nu_t) - K_{\mathcal{L}}^*(\nu_t)) \mu_t(\bar{\ell}_A) = 0 \quad (A)$$

*a.s.- $\mathbb{P}^{\mathcal{R}}$ , and provided that  $\theta_t = \theta_1$  for all  $t$ ,*

$$\lim_{t \rightarrow \infty} \int_{\Theta_k} (K(\bar{\theta}, \nu_t) - K_{\Theta_k}^*(\nu_t)) \rho_t^{(k)}(d\bar{\theta}) = 0 \quad (B)$$

*a.s.- $\mathbb{P}^{\mathcal{R}}$ , where  $(K_{\mathcal{L}}^*, K_{\Theta_k}^*)$  denote the minimal values of (18) and  $\mathbb{P}^{\mathcal{R}}$  is a probability measure over the set of realizable histories  $\mathbf{h} \in \mathcal{H}_D \times \mathcal{H}_A$  that is induced by  $(\pi_{\mathbf{h}_t})_{t \geq 1}$ .*

<sup>1</sup>We use the standard convention that  $-\ln 0 = \infty$  and  $0 \ln 0 = 0$ .

*Proof.* See Appendices C–D.  $\square$

Theorem 4 states that the conjectures produced by Alg. 1 are asymptotically consistent (18). This asymptotic consistency means that, if the sequence  $(\pi_{\mathbf{h}_t}, \nu_t)_{t \geq 1}$  generated by Alg. 1 converges, then it converges to an equilibrium of the following form.

**Definition 2** (Berk-Nash equilibrium, adapted from [50]).  $(\pi, \nu) \in \Pi \times \Delta(\mathcal{B})$  is a Berk-Nash equilibrium of  $\Gamma_{\theta_t}$  (Prob. 1, Alg. 1) iff there exist a  $\rho^{(k)} \in \Delta(\Theta_k)$  for each player  $k \in \{D, A\}$  such that

- (i) BOUNDED RATIONALITY.  $\pi_k$  is a best response against  $\pi_{-k}$  for any  $\mathbf{b}$  given  $(\nu, \rho^{(k)}, \rho^{(-k)})$ ,  $(\ell_k, \ell_{-k})$ , and  $\pi_1$ .
- (ii) CONSISTENCY.  $\rho^{(k)} \in \Delta(\Theta_k^*(\nu))$ .
- (iii) STATIONARITY.  $(\pi, \nu)$  is a limit point of some sequence  $(\pi_{\mathbf{h}_t}, \nu_t)_{t \geq 1}$  generated by Alg. 1, satisfying

$$\nu(\mathbf{b}') = \int_{\mathcal{B}} \mathbb{E}_{A^{(D)}, O, \Gamma_{\hat{\theta}}} \left[ \delta_{\mathbf{b}'}(\mathbb{B}(\mathbf{b}, A^{(D)}, O, \pi_A)) \right] d\nu(\mathbf{b}),$$

where  $\mathbb{B}$  is the belief operator defined in (6) and  $\Gamma_{\hat{\theta}}$  is parameterized by  $\hat{\theta} \triangleq \int_{\Theta_D} \hat{\theta} d\rho^{(D)}(\hat{\theta})$ .

**Corollary 1.**

- (A) If the sequence  $(\pi_{\mathbf{h}_t}, \nu_t)_{t \geq 1}$  generated by Alg. 1 converges to  $(\pi, \nu)$ , then  $(\pi, \nu)$  is a Berk-Nash equilibrium (Def. 2)
- (B) Given a Berk-Nash equilibrium  $(\pi, \nu)$  and assuming

$$\begin{aligned} \bar{\theta}^{(k)} \in \Theta_k^*(\nu) &\implies \mathbb{P}[\mathbf{I}^{(k)} | \bar{\theta}^{(k)}, \mathbf{b}] = \mathbb{P}[\mathbf{I}^{(k)} | \theta, \mathbf{b}] \quad (19a) \\ \ell_D = \ell_A = \infty, &\quad (19b) \end{aligned}$$

then  $(\pi, \mathbb{B})$  is a perfect Bayesian equilibrium (Def. 1).

*Proof.* Condition (i) in Def. 2 is ensured by rollout (13); condition (ii) is ensured asymptotically by Thm. 4; and condition (iii) is a consequence of convergence. Hence, statement (A) holds. Now consider statement (B). Condition 2) in Def. 1 is satisfied by definition of  $\mathbb{B}$  (6). To see why condition 1) also must hold, note that assumption (19a) together with condition (ii) of Def. 2 implies that  $\mathbb{P}[\mathbf{I}^{(k)} | \theta, \mathbf{b}] = \mathbb{P}[\mathbf{I}^{(k)} | \bar{\theta}^{(k)}, \mathbf{b}]$  for any  $\bar{\theta}^{(k)} \sim \rho^{(k)}$ . Consequently, it follows from assumption (19b) that  $\pi_A \in \mathcal{B}_A(\pi_D)$  and  $\pi_D \in \mathcal{B}_D(\pi_A)$  for any  $\mathbf{b}_1$  (9).  $\square$

Corollary 1 states that if the sequence  $(\pi_{\mathbf{h}_t}, \nu_t)_{t \geq 1}$  generated by Alg. 1 converges, then it must converge to a Berk-Nash equilibrium. Further, under the conditions defined in (19), this equilibrium is also a perfect Bayesian equilibrium (Def. 1). The converse is not necessarily true, however, since the perfect Bayesian equilibrium does not enforce condition (iii) of the Berk-Nash equilibrium (Def. 2). This condition requires that  $\nu_t$  converges to a stationary distribution, which is not guaranteed to exist. We provide an example in Appendix E.

## VI. DIGITAL TWIN AND SYSTEM IDENTIFICATION

To implement and evaluate the method described above for the APT use case (§II), we first estimate the parameters of  $\Gamma$  (1) using a digital twin of the target infrastructure shown in Fig. 1.

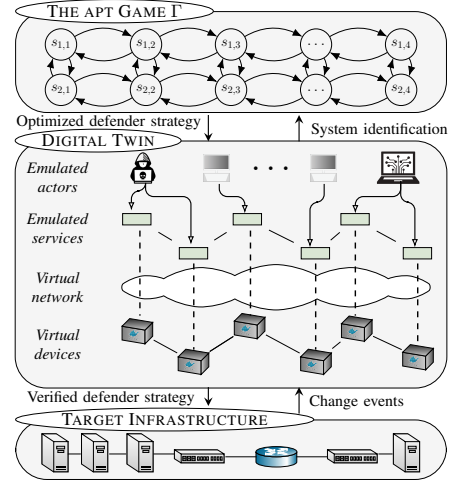


Fig. 10: The digital twin is a virtual replica of the target infrastructure; we use the twin for evaluation and data collection [34].

### A. Creating a Digital Twin of the Target Infrastructure

The configuration of the target infrastructure is listed in Appendix G. The topology is shown in Fig. 1. It consists of  $N = 64$  servers, some of which are vulnerable to APTs.

We create a digital twin of the target infrastructure using an open-source emulation system, which emulates servers with Linux containers and emulates network connectivity with Linux bridges [34]. Using this twin, we emulate the attacker using the actions listed in Table 2 and we emulate the defender through hypervisor-based recovery of servers [51].

### B. Estimating the Observation Distribution

Following the APT use case described in §II, we define the observation  $o_t$  (4) to be the priority-weighted sum of the number of IDS alerts at time  $t$ . For the evaluation reported in this paper, we collect about  $M = 10^5$  measurements of  $o_t$  in the digital twin (the measurements are available at [34], where  $|\mathcal{O}| = 26178$ ). Using these measurements, we estimate the observation distribution  $z$  (4) with the empirical distribution  $\hat{z}$ , where  $\hat{z} \xrightarrow{\text{a.s.}} z$  as  $M \rightarrow \infty$  (Glivenko-Cantelli theorem).

## VII. EXPERIMENTAL EVALUATION OF OUR METHOD

We implement our method (Fig. 7, Alg. 1) in Python and evaluate it through simulation studies based on measurements from the digital twin (Fig. 10). The source code of our implementation is available at [34]. The simulation environment runs on a server with a 24-core INTEL XEON GOLD 2.10 GHz CPU and 768 GB RAM. Hyperparameters for Alg. 1 and  $\Gamma$  (1) are listed in Appendix F.

### A. Evaluation Scenarios

We define four scenarios to evaluate the performance properties of our method (Fig. 7, Alg. 1). Our aim in evaluating these scenarios is to assess the following: a) the computational requirements of rollout (13); and b) the convergence rate of Alg. 1 for different instantiations of  $\Gamma_{\theta_t}$  (Prob. 1).

Type	Actions
Reconnaissance	TCP SYN scan, UDP port scan, TCP XMAS scan VULSCAN vulnerability scanner, ping-scan
Brute-force	TELNET, SSH, FTP, CASSANDRA, IRC, MONGODB, MYSQL, SMTP, POSTGRES
Exploit	CVE-2017-7494, CVE-2015-3306, CVE-2010-0426, CVE-2015-5602, CVE-2015-1427 CVE-2014-6271, CVE-2016-10033 CWE-89 weakness on the web app DVWA [52]

TABLE 2: Attacker actions on the digital twin (§II); when the attacker takes the stop action (§III-A), a randomly selected action is applied to every reachable server; actions are identified by the vulnerability identifiers in the Common Vulnerabilities and Exposures (CVE) database [53] and the Common Weakness Enumeration (CWE) list [54].

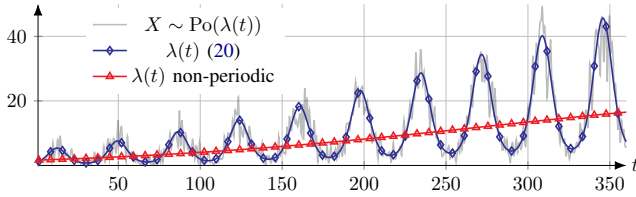


Fig. 11: The arrival rate function (20) used in Scenario 2; the blue curve shows the arrival rate  $\lambda(t)$ ; the red curve shows the trend of  $\lambda(t)$  without the periodic effects; and the shaded black curve shows the number of arrivals.

**Scenario 1** (Defender is uncertain about  $\ell_A$ ). In this scenario, the game is stationary (i.e.,  $\theta_t = \theta_1$  for all  $t$ ) and  $\theta_1$  is known to both players (i.e.,  $\rho_1^{(k)}(\theta_1) = 1$ ), but the defender is uncertain about the attacker’s lookahead horizon  $\ell_A$ , i.e.,  $\mu_1(\ell_A) < 1$ .

**Scenario 2** (Non-stationary  $\theta_t$ ). In this scenario,  $\ell_A$  is known to the defender but the game is non-stationary and  $z$  (4) is parameterized by  $\theta_t$ , which represents the number of clients. Clients arrive following a Poisson process with the following rate function (see Figs. 11–12) [55]

$$\lambda(t) = \exp \left( \underbrace{\sum_{i=1}^{\dim(\psi)} \psi_i t^i}_{\text{trend}} + \underbrace{\sum_{k=1}^{\dim(\chi)} \chi_k \sin(\omega_k t + \phi_k)}_{\text{periodic}} \right). \quad (20)$$

**Scenario 3** (Misspecified model conjectures  $\rho_t^{(D)}, \rho_t^{(A)}$ ). In this scenario, the game is stationary (i.e.,  $\theta_t = \theta_1$  for all  $t$ ) and  $\theta_1$  represents the compromise probability  $p_A$  (2). Further, the attacker’s lookahead horizon  $\ell_A$  is known to the defender but both players are uncertain about  $\theta_1$  and have misspecified conjectures, i.e.,  $\theta_1 \notin \Theta_A \cup \Theta_D$ .

**Scenario 4** (Defender is uncertain about  $\ell_A$  and  $\theta_t$ ). This scenario is the same as Scenario 3, except that the defender is uncertain about the attacker’s lookahead horizon  $\ell_A$ , i.e.,  $\mu_1(\ell_A) < 1$ .

## B. Evaluation Results (Fig. 13)

**Scenario 1.** Figures 13.a–b show the evolution of the defender’s conjecture distribution  $\mu_t$  (16b) and the discrepancy

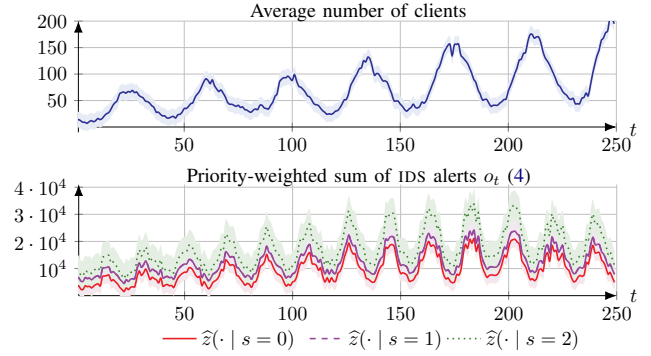


Fig. 12: Estimated distributions of the number of clients and the priority-weighted sum of IDS alerts ( $o_t$ ) during different arrival rates  $\lambda(t)$  based on the APT actions listed in Table 2 and the rate function shown in Fig. 11; the curves indicate mean values and the shaded areas indicate standard deviations from 3 measurements.

(17) of the conjecture  $\bar{\ell}_{A,t}$  when  $\mathcal{L} = \{1, 2\}$  and  $\ell_A = 1$ . We observe that  $\mu_t$  converges and concentrates on the consistent conjecture (18) after 5 time steps, as predicted by Thm. 4.A. Figure 13.d shows the rate of convergence for different  $|\mathcal{L}|$ , indicating that a larger  $|\mathcal{L}|$  leads to a slower convergence. This is expected since a larger  $|\mathcal{L}|$  means that the defender has a higher degree of uncertainty about  $\ell_A$ .

Figure 13.c shows the expected cost of the defender as a function of  $|\ell_A - \bar{\ell}_{A,t}|$ , which quantifies the inaccuracy of the defender’s conjecture  $\bar{\ell}_{A,t}$ . We observe that the cost of the defender is increasing with the inaccuracy of its conjecture. Next, Fig. 13.e shows the evolution of the discrepancy (17) of different conjectures. We observe that the discrepancies of the incorrect conjectures increase over time and that the discrepancy of the correct conjecture is 0 (by definition).

Lastly, Fig. 13.f shows the expected cost of Alg. 1 and the expected cost of best response reinforcement learning with CEM [39] (i.e., *best response dynamics* [56]). We note that the expected cost of reinforcement learning oscillates. Similar behavior of reinforcement learning has been observed in related work [32], [57]. By contrast, the expected cost of Alg. 1 is significantly more stable and its behavior is consistent with convergence to a Berk-Nash equilibrium (Def. 2).

**Scenario 2.** Figures 13.g–h show the evolution of the defender’s conjecture distribution  $\rho_t^{(D)}$  (16a) and the discrepancy (17) of the conjecture  $\bar{\theta}_t^{(D)}$  when  $\Theta_D = \{12, 9\}$  and  $\theta_t = 12$  for all  $t$ . We observe that  $\rho_t^{(D)}$  converges and concentrates on the consistent conjecture (18) after 18 time steps, as predicted by Thm. 4.B. Figure 13.j shows the rate of convergence for varying  $|\Theta_D|$ . As expected, when the defender’s uncertainty about  $\theta_t$  increases (i.e., when  $|\Theta_D|$  increases), the time it takes for the sequence of conjectures to converge increases.

Figure 13.i shows the expected cost of the defender as a function of  $|\theta_t - \bar{\theta}_t^{(D)}|$ , which quantifies the inaccuracy of the defender’s conjecture  $\bar{\theta}_t^{(D)}$ . We observe that the cost of the defender is increasing with the inaccuracy of its conjecture. Lastly, Figs. 13.k–l show the expected discrepancy (17) of the posterior (16a) when  $\theta_t$  is changing at every time step, whereby  $\rho_t^{(D)}$  does not converge. (Note that Thm. 4 only

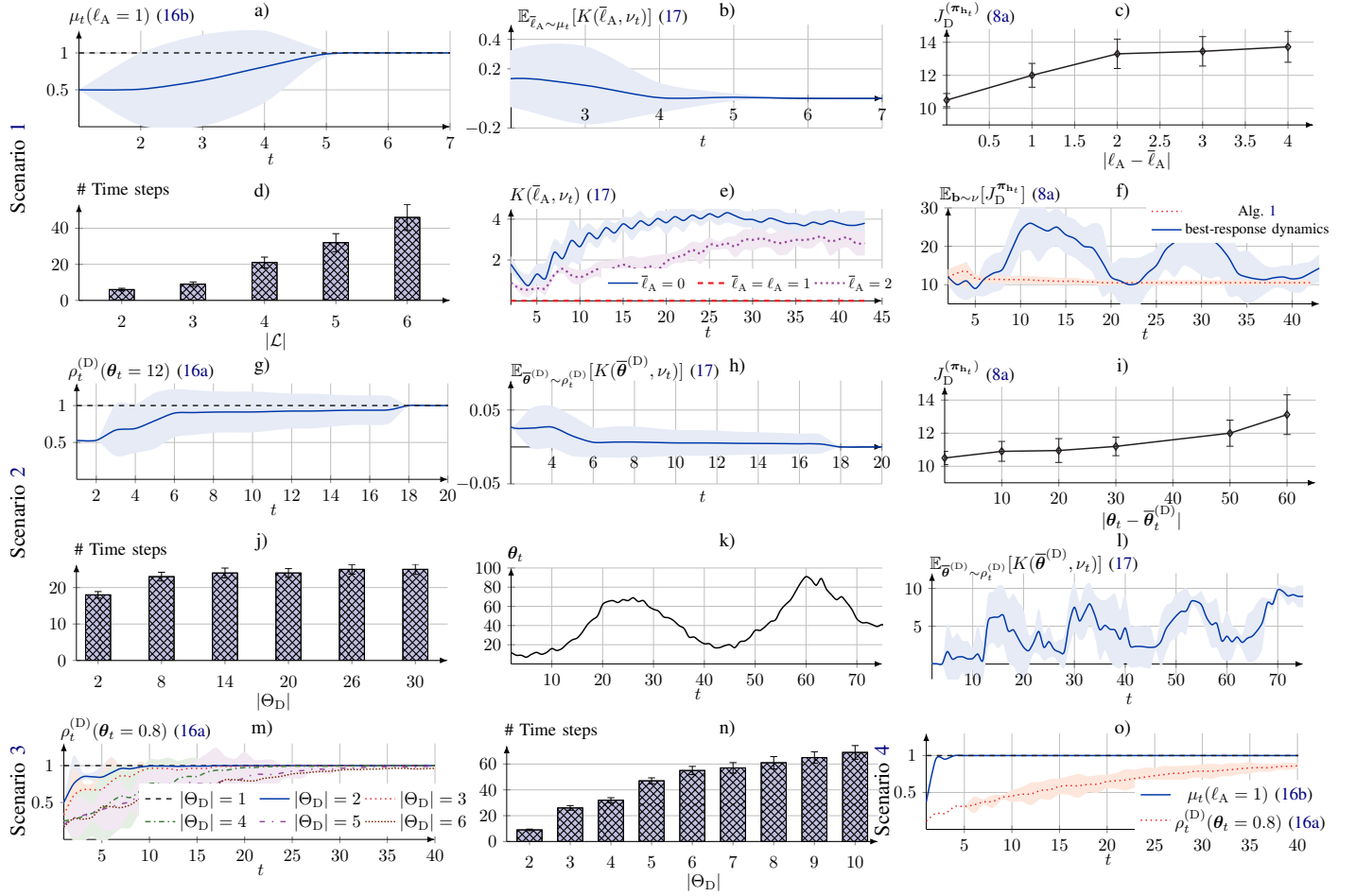


Fig. 13: Evaluation results; a)–f) relate to Scenario 1; g)–l) relate to Scenario 2; m)–n) relate to Scenario 3; and o) relate to Scenario 4; values indicate the mean; the shaded areas and the error bars indicate the 95% confidence interval based on 20 random seeds; hyperparameters are listed in Appendix F.

applies when  $\theta_t$  remains fixed.)

**Scenario 3.** Figures 13.m–n show the time for the defender’s conjecture  $\bar{\theta}_t^{(D)}$  to converge for different sizes of  $\Theta_D$  when  $\theta_t$  is fixed. We observe that the time to converge increases with the size of  $\Theta_D$ , which is expected since the size of  $\Theta_D$  represents the defender’s degree of uncertainty about  $\theta_t$ . Figure 14 shows the evolution of  $\rho_t^{(D)}$ . We observe that  $\rho_t^{(D)}$  starts from a uniform distribution over  $\Theta_D$  and as  $t \rightarrow \infty$ , it concentrates on the set of consistent conjectures  $\Theta_D^*$  (18a).

**Scenario 4.** Figure 13.o shows the evolution of the defender’s conjecture distributions  $\mu_t$  and  $\rho_t^{(D)}$  (16). We see in the figure that both distributions converge, which is consistent with Thm. 4. The convergence of  $\mu_t$  is significantly faster than that of  $\rho_t^{(D)}$ . We believe this difference is because  $|\mathcal{L}| < |\Theta_D|$ , which means that the defender is more uncertain about  $\ell_A$  than about  $\theta_t$ .

**Comparison with baselines.** The convergence times of our method (Alg. 1) and those used in prior work are listed in Table 3. While we observe that our method converges faster than the baselines, a direct comparison is not feasible for two reasons. First, the baselines do not consider the same solution concept as us, i.e., the Berk-Nash equilibrium (Def. 2). Second, the

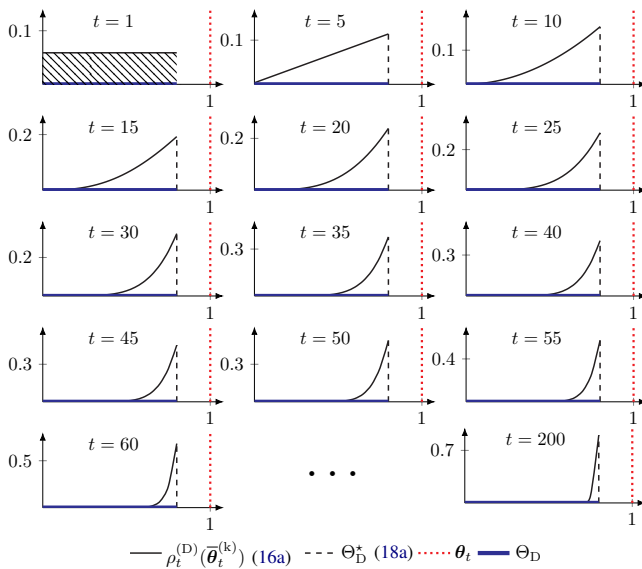


Fig. 14: Evolution of  $\rho_t^{(D)}$  (16a) when  $\Theta_D = \{0.0, 0.05, \dots, 0.8\}$  and  $\theta_t = 1$  for all  $t$  (Scenario 3); hyperparameters are listed in Appendix F.

Method	Fixed point	Time (min)
Alg. 1, $ \mathcal{L}  = 2,  \Theta_k  = 1$	Berk-Nash equilibrium (Def. 2)	$6.7 \pm 0.7$
Alg. 1, $ \mathcal{L}  = 3,  \Theta_k  = 1$	Berk-Nash equilibrium (Def. 2)	$11.4 \pm 0.9$
Alg. 1, $ \mathcal{L}  = 4,  \Theta_k  = 1$	Berk-Nash equilibrium (Def. 2)	$39.1 \pm 1.3$
Alg. 1, $ \mathcal{L}  = 4,  \Theta_k  = 1$	Berk-Nash equilibrium (Def. 2)	$137.3 \pm 2.8$
Alg. 1, $ \mathcal{L}  = 1,  \Theta_k  = 2$	Berk-Nash equilibrium (Def. 2)	$12.9 \pm 0.9$
Alg. 1, $ \mathcal{L}  = 1,  \Theta_k  = 32$	Berk-Nash equilibrium (Def. 2)	$17.9 \pm 1.0$
Alg. 1, $ \mathcal{L}  = 1,  \Theta_k  = 192$	Berk-Nash equilibrium (Def. 2)	$29.9 \pm 1.2$
Alg. 1, $ \mathcal{L}  = 4,  \Theta_k  = 192$	Berk-Nash equilibrium (Def. 2)	$194.6 \pm 3.7$
Best-response dynamics (Fig. 13.f)	$\epsilon$ -Nash equilibrium [40, Eq. 1]	DNC
HSVI [46, Alg. 1] (Fig. 6)	$\epsilon$ -Nash equilibrium [40, Eq. 1]	DNC
NFSP [60, Alg. 9]	$\epsilon$ -Nash equilibrium [40, Eq. 1]	$\approx 919$ min
Fictitious play [58]	$\epsilon$ -Nash equilibrium [40, Eq. 1]	$\approx 4800$ min
PPO [59, Alg. 1], static $\pi_A$	Best response (9a)	$9.2 \pm 0.4$ min

TABLE 3: Comparison with baseline methods in terms of speed of convergence; DNC is short for “does not converge”; “ $\approx$ ” means that the algorithm nearly converges; numbers indicate the mean and the standard deviation from evaluations with 3 random seeds; hyperparameters are listed in Appendix F.

baselines make different assumptions about the computational capacity and information available to the players. For example, fictitious play [58], which is a popular method among prior work, assumes that players a) have correctly specified models and b) have unlimited computational capacity. Similarly, popular reinforcement learning methods, such as PPO [59, Alg. 1] and NFSP [60, Alg. 9], are designed for offline rather than online learning.

### C. Discussion of the Evaluation Results

The key findings from the evaluation can be summarized as follows.

- (i) The conjectures produced by our method converges to consistent conjectures once the model parameters  $\theta_t$  remain fixed (18) (Figs. 13.a,g,m,o, Thm. 4). The rate of convergence decreases as  $|\mathcal{L}|$  and  $|\Theta_k|$  increase (Figs. 13.d,j,n).
- (ii) The cost of the defender increases as the distance between its conjecture and the true model increases (Figs. 13.c,i).
- (iii) Algorithm 1 allows to configure the computational capacity and the uncertainty of each player  $k$  by tuning  $\ell_k$  (Fig. 9) and  $(\mathcal{L}, \Theta_k)$ , respectively (Fig. 13).
- (iv) Algorithm 1 leads to effective strategies (Thm. 3) that are more stable than those obtained through reinforcement learning (Fig. 13.f, Table 3).
- (v) Computation of perfect Bayesian equilibria (Def. 1) and computation of exact rollout strategies is intractable for any non-trivial instantiation of  $\Gamma$  (Fig. 6, Fig. 9a).
- (vi) Approximate best response and rollout strategies of  $\Gamma$  can be efficiently computed using stochastic approximation (Fig. 9b, Fig. 4, Thm. 1).

The above findings suggest that our method can produce effective security strategies without relying on a correctly specified model of the environment. The practical implication of this result is that our method is suitable for dynamic IT infrastructures with short update cycles, which aligns with current trends of virtualization and zero-touch management.

## VIII. RELATED WORK

Since the early 2000s, researchers have studied automated security through modeling attacks and response actions on

an IT infrastructure as a game between an attacker and a defender (see textbooks [5], [61], [62]). The game is modeled in different ways depending on the use case. Examples include: APT games [2], [3], honeypot placement games [6], [7], resource allocation games [63], distributed denial-of-service games [64], [65], jamming games [66], and intrusion response games [8], [9], [32], [67]–[70]. These games are formulated using various models from the game-theoretic literature. For example: stochastic games (see e.g., [66]–[68]), extensive-form games (see e.g., [61]), Blotto games (see e.g., [63]), hypergames (see e.g., [23], [24]), POSGs (see e.g., [32], [65]), Stackelberg games (see e.g., [65], [70]), and evolutionary games (see e.g., [69]).

The main difference between this paper and the works referenced above is that we propose a method that allows to model non-stationary security games where players have probabilistic conjectures about the game model, which may be misspecified. By contrast, most of the referenced works assume that players have correctly specified models.

While the study of learning with misspecified models has attracted long-standing interest in economics [13], engineering [14], and psychology [15], it remains unexplored in the security context. Related research in the security literature include a) game-theoretic approaches based on bounded rationality; and b) model-free learning approaches. In the following subsections, we describe how these two approaches relate to this paper, where the main differences are listed in Table 4.

### A. Security Games with Bounded Rationality

Research on security games with bounded rationality includes [11], [19]–[21], [23]–[26]. These works differ from this paper in three main ways. First, they do not consider model misspecification as we do in this paper. Second, they study different types of games, i.e., one-stage games [11], [21]; network interdiction games [19]; differential games [26]; Stackelberg games [20]; behavioral games [26]; and hypergames [23], [24]. Third, they study different types of equilibria, i.e., Nash equilibria [25]; Gestalt Nash equilibria [11], [21]; Stackelberg equilibria [19], [20]; and Hyper Nash equilibria [23], [24]. By contrast, we study Berk-Nash equilibria [13, Def. 1] and a POSG where players have misspecified models. The benefit of our game model and equilibrium concept is that they better capture the APT use case (§II).

### B. Learning in Security Games

Prior work that study learning in security games includes [4], [8], [9], [31]–[33], [68], [71]–[73]. This paper differs from these works in two main ways. First, we design a novel way to update strategies using rollout with a conjectured model. This contrasts with all of the referenced works which consider other types of strategy updates, e.g., offline learning [8], [9], [73], meta-learning [31], model-free learning [32], [33], [68], [74], [75], and learning with perfect rationality [71], [72]. The advantage of our approach is that it allows to model players with limited computational capacity and varying degrees of misspecification. Second, we design a convergent Bayesian mechanism for online learning. In comparison, most of the

Paper	Use case	Method	Equilibrium	Evaluation	Game type
[70] Zonouz, 2009	Intrusion response	Dynamic programming	-	Testbed	Stationary POSG
[68] Zhu, 2009	Intrusion detection	Q-learning	Nash	Simulation	Stationary stochastic dynamic game
[71] Balcan, 2015	Resource allocation	No-regret learning	-	Analytical	Stationary repeated Stackelberg game
[72] Lisý, 2016	Resource allocation	No-regret learning	Nash	Analytical	Stationary NFGSS
[11] Chen, 2019	Risk management	Proximal optimization	Gestalt Nash	Simulation	Stationary one-stage game
[19] Sanjab, 2020	Drone operation	Prospect theory	Stackelberg	Simulation	Stationary network interdiction game
[24] Bakker, 2020	Intrusion response	Analytical	Hyper Nash	Simulation	Stationary repeated hypergame
[25] Abdallah, 2020	Power grid	Analytical	Nash	Simulation	Stationary behavioral game
[73] Huang, 2020	APT	Optimization	Perfect Bayes Nash	Simulation	Stationary POSG
[10] Zhao, 2020	Intrusion response	Analytical	Nash	Simulation	Non-stationary Markov game
[64] Aydeger, 2021	DDOS	Optimization	Perfect Bayes Nash	Testbed	Stationary signaling game
[23] Wan, 2022	APT	Analytical	Hyper Nash	Simulation	Stationary hypergame
[20] Gabrys, 2023	Cyber deception	Analytical	Stackelberg	Simulation	Stationary Stackelberg game
[8] Hammar, 2023	Intrusion response	Fictitious play	Nash	Testbed	Stationary POSG
[26] Mavridis, 2023	Cyber-physical security	Stochastic approximation	Nash	Simulation	Stationary differential game
[31] Ge, 2023	Zero-trust	Meta-learning	-	Simulation	Stationary POMDP
<b>This paper, 2024</b>	APT	Bayesian learning & rollout	Berk-Nash	Testbed & simulation	Non-stationary and misspecified POSG

TABLE 4: Comparison between this paper and related work.

prior work considers other types of learning mechanisms, e.g., fictitious play [8], [9], reinforcement learning [32], [33], [68], [74], [75], and no-regret learning [71], [72].

## IX. CONCLUSION AND FUTURE WORK

This paper presents a new game-theoretic method for online learning of security strategies that is applicable to dynamic IT environments where attacker and defender are uncertain about the environment and the opponent’s strategy. We formulate the interaction between an attacker and a defender as a non-stationary game where each player has a probabilistic conjecture about the game model, which may be misspecified in the sense that the true model has probability 0. Both players iteratively adapt their conjecture using Bayesian learning and update their strategy using rollout. We prove that the conjectures converge to best fits (Thm. 4), and we provide a bound on the performance improvement that rollout enables with a conjectured model (Thm. 3). To characterize the steady state of the game, we propose a novel equilibrium concept based on the Berk-Nash equilibrium, which represents a stable point where each player acts optimally given its conjecture (Def. 2). We present our method through an APT use case (§III). Simulation studies based on testbed measurements show that our method produces effective security strategies that adapt to a changing environment (Fig. 13). We also find that it leads to faster convergence than current reinforcement learning techniques (Table 3).

This paper opens up for several directions of future work. One direction is to extend our method and make it applicable to additional use cases. In particular, this paper considers an attacker with inside information – in future work we plan to investigate use cases with less capable attackers. Another direction of future work is to complement our asymptotic results (Thm. 4) with finite sample bounds, and to relate our definition of the Berk-Nash equilibrium (Def. 2) with other equilibrium concepts.

## X. ACKNOWLEDGMENTS

The authors would like to thank Forough Shahab Samani and Xiaoxuan Wang for their constructive comments on a

draft of this paper. The authors are also grateful to Branislav Bosanský for sharing the code of the HSVI algorithm.

## APPENDIX A PROOF OF THEOREM 1

Given  $(\pi_A, \pi_D)$ , the best response strategies  $(\tilde{\pi}_D, \tilde{\pi}_A)$  are optimal strategies in two POMDPs  $\mathcal{M}_D^P$  and  $\mathcal{M}_A^P$ . Hence, it suffices to show that there exists optimal strategies  $(\pi_D^*, \pi_A^*)$  in  $\mathcal{M}_D^P$  and  $\mathcal{M}_A^P$  that satisfy (10a) and (10b). Towards this proof, we state the following five lemmas.

**Lemma 1.**  $\mathcal{M}_D^P$  can be formulated as a repeated optimal stopping problem.

*Proof.* By definition, any optimal strategy  $\pi_D^*$  in  $\mathcal{M}_D^P$  satisfies

$$\begin{aligned} \pi_D^* &\in \arg \min_{\pi_D \in \Pi_D} \mathbb{E}_{(\pi_D, \pi_A)} \left[ \sum_{t=1}^{\infty} \gamma^{t-1} c(S_t, A_t^{(D)}) \mid S_1 = 0 \right] \\ &\stackrel{(a)}{=} \arg \min_{\pi_D \in \Pi_D} \left[ \mathbb{E}_{(\pi_D, \pi_A)} \left[ \sum_{t=1}^{\tau_1} \gamma^{t-1} c(S_t, A_t^{(D)}) \mid S_1 = 0 \right] + \right. \\ &\quad \left. \mathbb{E}_{(\pi_D, \pi_A)} \left[ \sum_{t=\tau_1+1}^{\tau_2} \gamma^{t-1} c(S_t, A_t^{(D)}) \mid S_{\tau_1} = 0 \right] + \dots \right] \\ &\stackrel{(b)}{=} \arg \min_{\pi_D \in \Pi_D} \left[ \mathbb{E}_{(\pi_D, \pi_A)} \left[ \sum_{t=1}^{\tau_1} \gamma^{t-1} c(S_t, A_t^{(D)}) \mid S_1 = 0 \right] \right], \end{aligned}$$

where  $\tau_1, \tau_2, \dots$  are the stopping times; (a) follows by linearity of expectation; and (b) follows because all elements inside the infinite sum are equivalent up to a constant factor.  $\square$

**Lemma 2.** The optimal cost-to-go function  $J_D^*(\mathbf{b})$  in  $\mathcal{M}_D^P$  is piecewise linear and concave with respect to  $\mathbf{b} \in \mathcal{B}$ .

*Proof.* This property was originally proven by E.J. Sondik [76, Thm. 2]. A more accessible version of the proof can be found in [38, Thms. 7.6.1–7.6.2]. For brevity we omit it here.  $\square$

**Lemma 3.** Let  $\mathcal{S} \subseteq \mathcal{B}$  denote the subset of the belief space in  $\mathcal{M}_D^P$  where it is optimal to stop, i.e.,  $\mathbf{b} \in \mathcal{S} \iff \pi_D^*(\mathbf{b}) = S$ . If  $N = 1$ , then  $\mathcal{S}$  is a convex set.

*Proof.* As  $N = 1$ , we have that  $\mathcal{B} = [0, 1]$  and  $b_t = \mathbb{P}[S_t = 1 \mid \mathbf{h}_t^{(D)}]$ . To show that  $\mathcal{S}$  is convex, we need to show that

$b_1, b_2 \in \mathcal{S} \implies \lambda b_1 + (1 - \lambda)b_2 \in \mathcal{S}$  for any  $\lambda \in [0, 1]$ . Since  $J_D^*(b)$  is concave (Lemma 2), we have

$$J_D^*(\lambda b_1 + (1 - \lambda)b_2) \geq \lambda J_D^*(b_1) + (1 - \lambda)J_D^*(b_2).$$

As  $b_1, b_2 \in \mathcal{S}$  by assumption, the optimal action given  $b_1$  or  $b_2$  is  $S$ . Thus  $J_D^*(b_1) = Q_D^*(b_1, S)$  and  $J_D^*(b_2) = Q^*(b_2, S)$ , where  $Q_D^*$  is the optimal Q-function in  $\mathcal{M}_D^P$ . Since  $Q_D^*(b_t, S) = \mathbb{E}_{S_t}[c(S_t, S) \mid b_t] = bc(1, S) + (1 - b)c(0, S)$ , we obtain

$$\begin{aligned} J_D^*(\lambda b_1 + (1 - \lambda)b_2) &\geq \lambda J_D^*(b_1) + (1 - \lambda)J_D^*(b_2) \\ &\geq \lambda Q_D^*(b_1, S) + (1 - \lambda)Q_D^*(b_2, S) \\ &\geq \lambda(b_1 c(1, S) + (1 - b_1)c(0, S)) + \\ &\quad (1 - \lambda)(b_1 c(1, S) + (1 - b_1)c(0, S)) \\ &\geq (\lambda b_1 + (1 - \lambda)b_2)c(1, S) + (1 - (\lambda b_1 + (1 - \lambda)b_2))c(0, S) \\ &\geq Q_D^*(\lambda b_1 + (1 - \lambda)b_2, S) \\ &\stackrel{(a)}{\geq} J_D^*(\lambda b_1 + (1 - \lambda)b_2), \end{aligned}$$

where (a) follows because  $J_D^*$  is optimal. This shows that if  $b_1, b_2 \in \mathcal{S}$  then  $Q_D^*(\lambda b_1 + (1 - \lambda)b_2, S) = J_D^*(\lambda b_1 + (1 - \lambda)b_2)$ , which means that  $\lambda b_1 + (1 - \lambda)b_2 \in \mathcal{S}$  for any  $\lambda \in [0, 1]$ . Hence,  $\mathcal{S}$  is convex [38, Thm. 2.2.1].  $\square$

**Lemma 4.** *If  $s_t = N$ , then  $a_t^{(A)} = C$  is a best response for any  $\mathbf{b}_t \in \mathcal{B}$  and  $\pi_D \in \Pi_D$ .*

*Proof.* Assume by contradiction that  $a_t^{(A)} = C$  is not a best response. Then the expected cost of  $a_t^{(A)} = S$  must be lower than that of  $a_t^{(A)} = C$ , i.e.,

$$\begin{aligned} Q_A^*((\mathbf{b}_t, N), S) &< Q_A^*((\mathbf{b}_t, N), C) \stackrel{(a)}{\implies} -c(s_t, a_t^{(D)}) + \\ &\gamma^{t-1} \mathbb{E}_{A_t^{(D)}, O_t}[J_A^*(\mathbf{B}_{t+1}) \mid s_t = N, a_t^{(A)} = S] < -c(s_t, a_t^{(D)}) + \\ &\gamma^{t-1} \mathbb{E}_{A_t^{(D)}, O_t}[J_A^*(\mathbf{B}_{t+1}) \mid s_t = N, a_t^{(A)} = C] \stackrel{(b)}{\implies} \\ &\mathbb{E}_{A_t^{(D)}} \left[ \sum_{o \in \mathcal{O}} z(o \mid \mathbf{b}_t, A^{(D)}) J_A^*(\mathbb{B}(\mathbf{b}_t, a_t^{(D)}, o_t, \pi_A)) \mid s_t = N \right] \\ &< \mathbb{E}_{A_t^{(D)}} \left[ \sum_{o \in \mathcal{O}} z(o \mid \mathbf{b}_t, A^{(D)}) J_A^*(\mathbb{B}(\mathbf{b}_t, a_t^{(D)}, o_t, \pi_A)) \mid s_t = N \right] \\ &\stackrel{(c)}{\implies} 0 < 0 \quad (\text{contradiction}), \end{aligned}$$

where  $Q_A^*((\mathbf{b}_t, N), S)$  is the optimal Q-function in  $\mathcal{M}_A^P$ ,  $\pi_A$  is the attacker strategy assumed by  $\pi_D$ , and  $\mathbb{B}$  is defined in (6). Step (a) follows from Bellman's optimality equation [77, Eq. 1]; (b) follows because  $c$  (7) is independent of  $a_t^{(A)}$ ; and (c) follows because both  $a_t^{(A)} = C$  and  $a_t^{(A)} = S$  lead to the same state when  $s_t = N$  (2).  $\square$

**Lemma 5.** *If  $\pi_D(S \mid \mathbf{b}_t) = 1$  for some  $\mathbf{b}_t \in \mathcal{B}$ , then  $a_t^{(A)} = C$  is a best response.*

*Proof.* Assume by contradiction that  $a_t^{(A)} = C$  is not a best response. Then the expected cost of  $a_t^{(A)} = S$  must be lower than that of  $a_t^{(A)} = C$ , i.e.,

$$\begin{aligned} Q_A^*((\mathbf{b}_t, s_t), S) &< Q_A^*((\mathbf{b}_t, s_t), C) \\ &\stackrel{(a)}{\implies} \gamma^{t-1} J_A^*(\mathbf{e}_1) < \gamma^{t-1} J_A^*(\mathbf{e}_1) \end{aligned}$$

$$\stackrel{(b)}{\implies} 0 < 0 \quad (\text{contradiction}),$$

where (a) follows because  $c$  (7) is independent of  $a_t^{(A)}$  and because  $\pi_D(S \mid \mathbf{b}_t) = 1 \implies \mathbf{b}_{t+1} = \mathbf{e}_1$  (2).  $\square$

#### A. Proof of Theorem 1.A

Lemma 3 and the assumption that  $N = 1$  means that  $\mathcal{S} = [\alpha^*, \kappa]$ , where  $0 \leq \alpha^* \leq \kappa \leq 1$ . Thus it suffices to show that  $\kappa = 1$ . Bellman's optimality equation [77, Eq. 1] implies that

$$\begin{aligned} \pi_D^*(1) &\in \arg \min_{a \in \{S, C\}} \left[ \overbrace{c(1, S)}^S, \overbrace{c(1, C) + \gamma J_D^*(1)}^C \right] \\ &\stackrel{(a)}{=} \arg \min_{a \in \{S, C\}} \left[ c(1, S), c(1, S) + \sum_{t=1}^{\tau} \gamma^t c(1, C) \right] \\ &\stackrel{(b)}{=} \arg \min_{a \in \{S, C\}} \left[ c(1, S), c(1, S) + \frac{1 - \gamma^{\tau-1}}{1 - \gamma} \right] = S, \end{aligned}$$

where  $\tau \geq 1$  denotes the stopping time. Step (a) follows because  $s = 1$  is an absorbing state and (b) follows from (7). As a consequence,  $\pi_D^*(1) = S \implies \mathcal{S} = [\alpha^*, 1]$ .  $\square$

#### B. Proof of Theorem 1.B

Since  $N = 1$ , we have that  $\mathcal{B} = [0, 1]$  and  $b_t = \mathbb{P}[S_t = 1 \mid \mathbf{h}_t^{(D)}]$ . Given Lemma 4, it suffices to consider the case when  $s_t = 0$ . From Lemma 5 and the assumption that  $\pi_D$  satisfies (10a), we know that  $a_t^{(A)} = S$  is a best response iff  $b_t \in [0, \alpha^*]$ , where  $\alpha^* \leq 1$ . It further follows from Lemma 5 that  $\alpha^* = 0 \implies \beta^* = 0$ . Thus Thm. 1.B holds when  $\alpha^* = 0$ . Now consider the case when  $\alpha^* > 0$ . We know from Lemma 4 and (7) that the difference in expected cost for the attacker when  $a_t^{(A)} = S$  and when  $a_t^{(A)} = C$  is negatively proportional to the next stopping time of the defender  $T^{(D)}$ . We will show that  $\mathbb{E}[T^{(D)}]$  is decreasing in  $b_t$ .

The transition matrices of  $\mathcal{M}_A^P$  are

$$\begin{matrix} & \begin{matrix} 0 & 1 \end{matrix} \\ \begin{matrix} 0 \\ 1 \end{matrix} & \begin{bmatrix} 1 & 0 \\ q & 1 - q \end{bmatrix} \end{matrix} \quad \text{and} \quad \begin{matrix} & \begin{matrix} 0 & 1 \end{matrix} \\ \begin{matrix} 0 \\ 1 \end{matrix} & \begin{bmatrix} q & 1 - q \\ q & 1 - q \end{bmatrix}, \quad (21)$$

where  $q \triangleq \pi_D(S \mid b_t)$ . The left matrix in (21) relates to  $a_t^{(A)} = C$  and the right matrix relates to  $a_t^{(A)} = S$ . The determinants of these matrices are  $(1 - q)$  and  $0$ , which means that they are TP-2 [38, Def. 10.2.1]. By assumption,  $z(o_t \mid s_t)$  (4) is also TP-2. This means that  $\mathbb{B}$  (6) is non-decreasing in  $b_t$  [38, Thm. 10.3.1]. Consequently,  $\mathbb{E}[T^{(D)}]$  is decreasing in  $b_t$ . Hence, if there is some  $b_t$  where  $a_t^{(A)} = S$  is a best response, then for any  $b'_t < b_t$ ,  $a_t^{(A)} = S$  must also be a best response. We know from Lemma 2 and Lemma 3 that the stopping set for the attacker is a convex subset  $[0, \beta^*] \subset [0, \alpha^*]$ . Thus there exists a threshold  $\beta^* \in [0, \alpha^*]$  such that  $a_t^{(A)} = S$  is a best response iff  $b_t > \beta^*$ .  $\square$

APPENDIX B  
PROOF OF THEOREM 3

As (13) implements one step of the policy iteration algorithm [78, Eqs. 6.4.1-22], (15a) follows from standard results in dynamic programming theory, see e.g., [47, Prop. 1].

To prove (15b) we adapt the proof in [79, Prop 5.1.1]. Let  $\bar{\pi} \triangleq (\pi_{k,t}, \bar{\pi}_{-k,t})$  and let  $\pi \triangleq (\pi_{k,1}, \bar{\pi}_{-k,t})$ . Then define

$$(T_{k,\pi} J_k)(\mathbf{b}_t) \triangleq \mathbb{E}_\pi[c(S_t, A_t^{(D)}) + \gamma J_k(\mathbf{B}_{t+1}) \mid \pi] \quad \forall \mathbf{b} \in \mathcal{B}.$$

Since  $J_k^{(\pi)}$  is a fixed point of  $T_{k,\pi}$ , i.e.,  $T_{k,\pi} J_k^{(\pi)} = J_k^{(\pi)}$ , and since  $T_{k,\pi}^k$  is a contraction mapping [78, Prop. 6.2.4], we have that  $\lim_{j \rightarrow \infty} T_{k,\pi}^j J_k^{(\pi)} = J_k^{(\pi)}$  for any  $J$  [78, Thm. 6.4.6, Cor. 6.4.7]. As a consequence

$$\|\bar{J}_k^{(\bar{\pi})} - J_k^*\| = \lim_{j \rightarrow \infty} \|T_{k,\bar{\pi}}^j J_k^* - J_k^*\|. \quad (22)$$

By repeated application of the triangle inequality:

$$\begin{aligned} \|T_{k,\bar{\pi}}^j J_k^* - J_k^*\| &\leq \|T_{k,\bar{\pi}}^j J_k^* - T_{k,\bar{\pi}}^{j-1} J_k^*\| + \|T_{k,\bar{\pi}}^{j-1} J_k^* - J_k^*\| \\ &\leq \dots \leq \sum_{m=1}^j \|T_{k,\bar{\pi}}^m J_k^* - T_{k,\bar{\pi}}^{m-1} J_k^*\|. \end{aligned}$$

Since  $T_{k,\bar{\pi}}$  is a contraction mapping with modulus  $\gamma < 1$ ,

$$\begin{aligned} \|T_{k,\bar{\pi}}(T_{k,\bar{\pi}} J_k^*) - T_{k,\bar{\pi}} J_k^*\| &\leq \gamma \|T_{k,\bar{\pi}} J_k^* - J_k^*\| \\ \implies \|T_{k,\bar{\pi}}^j J_k^* - T_{k,\bar{\pi}}^{j-1} J_k^*\| &\leq \gamma^{j-1} \|T_{k,\bar{\pi}} J_k^* - J_k^*\|. \end{aligned}$$

The above inequality means that

$$\sum_{m=1}^j \|T_{k,\bar{\pi}}^m J_k^* - T_{k,\bar{\pi}}^{m-1} J_k^*\| \leq \sum_{m=1}^j \gamma^{m-1} \|T_{k,\bar{\pi}} J_k^* - J_k^*\|.$$

Since non-strict inequalities are preserved by limits,

$$\begin{aligned} \lim_{j \rightarrow \infty} \|T_{k,\bar{\pi}}^j J_k^* - J_k^*\| &\leq \lim_{j \rightarrow \infty} \sum_{m=1}^j \gamma^{m-1} \|T_{k,\bar{\pi}} J_k^* - J_k^*\| \\ &= \frac{\|T_{k,\bar{\pi}} J_k^* - J_k^*\|}{1 - \gamma}. \end{aligned} \quad (23)$$

Now let  $\hat{J}_k^{(\bar{\pi})} \triangleq T_{k,\ell_k}^{\bar{\pi}_{-k,t}} \bar{J}_k^{(\bar{\pi})}$ , where  $T_{k,\ell_k}^{\bar{\pi}_{-k,t}}$  is defined in (13). Note that  $T_{k,\bar{\pi}} \hat{J}_k^{(\bar{\pi})} = T_{k,1}^{\bar{\pi}_{-k,t}} \hat{J}_k^{(\bar{\pi})}$  and  $T_{k,1}^{\bar{\pi}_{-k,t}} J_k^* = J_k^*$  by definition [12].

Applying the triangle inequality to the numerator in (23),

$$\begin{aligned} \|T_{k,\bar{\pi}} J_k^* - J_k^*\| &\leq \|T_{k,\bar{\pi}} J_k^* - T_{k,\bar{\pi}} \hat{J}_k^{(\bar{\pi})}\| + \\ \|T_{k,\bar{\pi}} \hat{J}_k^{(\bar{\pi})} - T_{k,1}^{\bar{\pi}_{-k,t}} \hat{J}_k^{(\bar{\pi})}\| &+ \|T_{k,1}^{\bar{\pi}_{-k,t}} \hat{J}_k^{(\bar{\pi})} - J_k^*\| \\ = \|T_{k,\bar{\pi}} J_k^* - T_{k,\bar{\pi}} \hat{J}_k^{(\bar{\pi})}\| &+ \|T_{k,1}^{\bar{\pi}_{-k,t}} \hat{J}_k^{(\bar{\pi})} - T_{k,1}^{\bar{\pi}_{-k,t}} J_k^*\| \\ &\leq \gamma \|\hat{J}_k^{(\bar{\pi})} - J_k^*\| \qquad \leq \gamma \|\hat{J}_k^{(\bar{\pi})} - J_k^*\| \\ \leq 2\gamma \|\hat{J}_k^{(\bar{\pi})} - J_k^*\| &= 2\gamma \|T_{k,\ell_k}^{\bar{\pi}_{-k,t}} \bar{J}_k^{(\bar{\pi})} - T_{k,\ell_k}^{\bar{\pi}_{-k,t}} J_k^*\| \\ \leq 2\gamma^{\ell_k} \|\bar{J}_k^{(\bar{\pi})} - J_k^*\|. \end{aligned} \quad (24)$$

Combining (22)–(24) gives (15b).  $\square$

APPENDIX C  
PROOF OF THEOREM 4.A

The idea behind the proof of Thm. 4.A. is to express  $\mu_t$  (16b) in terms of log-likelihood ratios, which can be shown to converge using the martingale convergence theorem [80, Thm. 6.4.3]. Towards this proof, we state the following two lemmas.

**Lemma 6.** Any sequence  $(\pi_{\mathbf{h}_t})_{t \geq 1}$  generated by Alg. 1 induces a well-defined probability measure  $\mathbb{P}^{\mathcal{R}}$  over the set of realizable histories  $\mathbf{h} \in \mathcal{H}_D \times \mathcal{H}_A$ .

*Proof.* Since the sample space of the random vectors  $(\mathbf{I}_t^{(D)}, \mathbf{I}_t^{(A)})$  (3) is finite (and measurable) for each  $t$ , the space of realizable histories  $\mathbf{h} \in \mathcal{H}_{D,t} \times \mathcal{H}_{A,t}$  is countable. By the Ionescu-Tulcea extension theorem it thus follows that a measure  $\mathbb{P}^{\mathcal{R}}$  over  $\mathcal{H}_{D,t} \times \mathcal{H}_{A,t}$  exists for  $t = 1, 2, \dots$  [81].  $\square$

**Lemma 7.** For any  $\bar{\ell}_A \in \mathcal{L}$  and any sequence  $(\nu_t, \pi_{\mathbf{h}_t})_{t \geq 1}$  generated by Alg. 1, the following holds a.s.- $\mathbb{P}^{\mathcal{R}}$  as  $t \rightarrow \infty$

$$\left| t^{-1} \sum_{\tau=1}^t \underbrace{\ln \frac{\mathbb{P}[\mathbf{i}_{\tau+1}^{(D)} \mid \ell_A, \mathbf{b}_\tau]}{\mathbb{P}[\mathbf{i}_{\tau+1}^{(D)} \mid \bar{\ell}_A, \mathbf{b}_\tau]}}_{\triangleq Z_{t+1}(\bar{\ell}_A)} - K(\bar{\ell}_A, \nu_t) \right| = 0.$$

*Proof.* By definition of  $Z_t$  and  $\nu_t$ ,

$$\begin{aligned} Z_{t+1}(\bar{\ell}_A) &= \sum_{\mathbf{b} \in \mathcal{B}} \sum_{\tau=1}^t t^{-1} \mathbb{1}_{\{\mathbf{b}\}}(\mathbf{b}_\tau) \ln \frac{\mathbb{P}[\mathbf{i}_{\tau+1}^{(D)} \mid \ell_A, \mathbf{b}_\tau]}{\mathbb{P}[\mathbf{i}_{\tau+1}^{(D)} \mid \bar{\ell}_A, \mathbf{b}_\tau]} \\ &= \mathbb{E}_{\mathbf{b} \sim \nu_t} \left[ \sum_{\tau=1}^t \frac{\ln \mathbb{P}[\mathbf{i}_{\tau+1}^{(D)} \mid \ell_A, \mathbf{b}]}{t} - \sum_{\tau=1}^t \frac{\ln \mathbb{P}[\mathbf{i}_{\tau+1}^{(D)} \mid \bar{\ell}_A, \mathbf{b}]}{t} \right]. \end{aligned}$$

This means that if the left sum above converges to  $\mathbb{E}_{\mathbf{I}^{(D)}}[\ln \mathbb{P}[\mathbf{I}^{(D)} \mid \bar{\ell}_A, \mathbf{b}]]$  and the right sum converges to  $\mathbb{E}_{\mathbf{I}^{(D)}}[\ln \mathbb{P}[\mathbf{I}^{(D)} \mid \ell_A, \mathbf{b}]]$ , we obtain  $Z_t \xrightarrow[t \rightarrow \infty]{} K(\bar{\ell}_A, \nu_t)$ , which yields the desired result. As these two proofs are almost identical we only provide the first proof here.

Let  $X_\tau \triangleq \ln \mathbb{P}[\mathbf{i}_{\tau+1}^{(D)} \mid \ell_A, \mathbf{b}_\tau] - \mathbb{E}_{\mathbf{I}^{(D)}}[\ln \mathbb{P}[\mathbf{I}^{(D)} \mid \ell_A, \mathbf{b}_\tau]]$ . We will show that  $(X_\tau)_{\tau \geq 1}$  is a martingale difference sequence (MDS). To show this, we need to prove that (i)  $\mathbb{E}[X_\tau \mid \mathbf{h}_{\tau-1}] = 0$ ; and (ii)  $\mathbb{E}[|X_\tau|] < \infty$ . We start with (i),

$$\begin{aligned} \mathbb{E}[X_\tau \mid \mathbf{h}_{\tau-1}] &= \mathbb{E}_{\mathbf{I}^{(D)}} \left[ \ln \mathbb{P}[\mathbf{I}^{(D)} \mid \ell_A, \mathbf{b}_\tau] - \mathbb{E}_{\mathbf{I}^{(D)}} \left[ \ln \mathbb{P}[\mathbf{I}^{(D)} \mid \ell_A, \mathbf{b}_\tau] \right] \mid \mathbf{h}_{\tau-1} \right] \\ &\stackrel{(a)}{=} \mathbb{E}_{\mathbf{I}^{(D)}} \left[ \ln \mathbb{P}[\mathbf{I}^{(D)} \mid \ell_A, \mathbf{b}_\tau] - \mathbb{E}_{\mathbf{I}^{(D)}} \left[ \ln \mathbb{P}[\mathbf{I}^{(D)} \mid \ell_A, \mathbf{b}_\tau] \right] \right] = 0, \end{aligned}$$

where (a) follows because  $\mathbf{I}^{(D)}$  is conditionally independent of  $\mathbf{h}_{\tau-1}$  given  $\mathbf{b}_\tau$  (5).

To prove (ii) we will write  $X_\tau$  as an expression of the form  $(\ln \mathbb{P}[\varphi])^2 \mathbb{P}[\varphi]$ , which is bounded by 1<sup>2</sup>. Towards this end, we start by applying Jensen's inequality to obtain

$$\mathbb{E}[|X_\tau|] = (\mathbb{E}[X_\tau^2])^{1/2} \leq (\mathbb{E}[X_\tau^2])^{1/2}, \quad (25)$$

which means that it suffices to bound  $\mathbb{E}[X_\tau^2]$ .

Next, we write  $\ln \mathbb{P}[\mathbf{i}_{\tau+1}^{(D)} \mid \ell_A, \mathbf{b}_\tau]$  as

$$\sum_{\mathbf{I}^{(D)}} \mathbb{1}_{\{\mathbf{I}^{(D)}\}}(\mathbf{i}_{\tau+1}^{(D)}) \frac{\mathbb{P}[\mathbf{I}^{(D)} \mid \ell_A, \mathbf{b}_\tau]}{\mathbb{P}[\mathbf{I}^{(D)} \mid \ell_A, \mathbf{b}_\tau]} \ln \mathbb{P}[\mathbf{I}^{(D)} \mid \ell_A, \mathbf{b}_\tau]$$

<sup>2</sup>We use the standard convention that  $(\ln 0)^2 0 = 0$ .

$$= \frac{\mathbb{E}_{\mathbf{I}^{(D)}} \left[ \mathbb{1}_{\{\mathbf{I}^{(D)}\}}(\mathbf{i}_{\tau+1}^{(D)}) \ln \mathbb{P}[\mathbf{I}^{(D)} | \ell_A, \mathbf{b}_\tau] \right]}{\mathbb{P}[\mathbf{i}_{\tau+1}^{(D)} | \ell_A, \mathbf{b}_\tau]},$$

which means that we can write  $X_\tau$  as

$$\mathbb{E}_{\mathbf{I}^{(D)}} \left[ \kappa \left( \mathbb{1}_{\{\mathbf{I}^{(D)}\}}(\mathbf{i}_{\tau+1}^{(D)}) - \mathbb{P}[\mathbf{i}_{\tau+1}^{(D)} | \ell_A, \mathbf{b}_\tau] \right) \middle| \ell_A, \mathbf{b}_\tau \right], \quad (26)$$

where  $\kappa \triangleq \ln \mathbb{P}[\mathbf{I}^{(D)} | \ell_A, \mathbf{b}_\tau]$ .

Since we focus on realizable histories, we have that  $\mathbb{P}[\mathbf{i}_{\tau+1}^{(D)} | \ell_A, \mathbf{b}_\tau] \in (0, 1]$ , which means that it is safe to suppress the denominator in (26). Consequently, the square of (26) can be bounded by the Cauchy-Schwarz inequality as

$$\leq \mathbb{E}_{\mathbf{I}^{(D)}} \left[ \underbrace{\kappa^2 \left( \mathbb{1}_{\{\mathbf{I}^{(D)}\}}(\mathbf{i}_\tau^{(D)}) + 1 \right) - \mathbb{P}[\mathbf{i}_{\tau+1}^{(D)} | \ell_A, \mathbf{b}_\tau]}_{\triangleq \chi} \middle| \ell_A, \mathbf{b}_\tau \right].$$

Next, since  $\kappa \geq 0$  and  $\chi \in [0, 1]$ , we obtain that

$$X_\tau^2 \leq \mathbb{E}_{\mathbf{I}^{(D)}} [\kappa^2 \chi^2 | \ell_A, \mathbf{b}_\tau] \leq \mathbb{E}_{\mathbf{I}^{(D)}} [\kappa^2 | \ell_A, \mathbf{b}_\tau],$$

which means that

$$\mathbb{E}[X_\tau^2] \leq \mathbb{E}_{\mathbf{I}^{(D)}} \left[ \mathbb{P}[\mathbf{I}^{(D)} | \ell_A, \mathbf{b}_\tau] \ln^2 \mathbb{P}[\mathbf{I}^{(D)} | \ell_A, \mathbf{b}_\tau] \middle| \ell_A, \mathbf{b}_\tau \right] \leq 1$$

$$\stackrel{(a)}{\implies} \mathbb{E}[|X_\tau|] \leq 1,$$

where (a) follows from (25). Therefore,  $(X_\tau)_{\tau \geq 1}$  is an MDS. Consequently, the sequence  $Y_t \triangleq \sum_{\tau=1}^t X_\tau$  is a martingale. By the martingale convergence theorem,  $(Y_\tau)_{\tau \geq 1}$  converges to a finite and integrable random variable a.s.- $\mathbb{P}^{\mathcal{L}}$  [80, Thm. 6.4.3]. This convergence means that we can invoke Kronecker's lemma, which states that  $\lim_{t \rightarrow \infty} t^{-1} \sum_{\tau=1}^t X_\tau = 0$  a.s.- $\mathbb{P}^{\mathcal{L}}$  [82, pp. 105]. As a consequence, the following holds a.s.- $\mathbb{P}^{\mathcal{L}}$  as  $t \rightarrow \infty$

$$\mathbb{E}_{\mathbf{b} \sim \nu_t} \sum_{\tau=1}^t \frac{\ln \mathbb{P}[\mathbf{i}_{\tau+1}^{(D)} | \ell_A, \mathbf{b}]}{t} = \mathbb{E}_{\mathbf{b} \sim \nu_t} \mathbb{E}_{\mathbf{I}^{(D)}} \left[ \ln \mathbb{P}[\mathbf{I}^{(D)} | \ell_A, \mathbf{b}] \right].$$

□

#### A. Proof of Theorem 4.A

To streamline analysis we treat  $\mu_t$  as a probability measure over  $\mathcal{L}$  and use integral language. From Bayes rule and the Markov property of  $\mathbb{P}[\mathbf{I}^{(D)} | \bar{\ell}_A, \mathbf{b}_t]$ , we have that

$$\begin{aligned} \mu_{t+1}(\bar{\ell}_A) &= \frac{\mathbb{P}[\bar{\ell}_A] \mathbb{P}[\mathbf{i}_2^{(D)}, \dots, \mathbf{i}_{t+1}^{(D)} | \bar{\ell}_A, \mathbf{h}_t^{(D)}]}{\mathbb{P}[\mathbf{i}_2^{(D)}, \dots, \mathbf{i}_{t+1}^{(D)} | \mathbf{h}_t^{(D)}]} \\ &\stackrel{(a)}{=} \frac{\mu_1(\bar{\ell}_A) \prod_{\tau=1}^t \mathbb{P}[\mathbf{i}_{\tau+1}^{(D)} | \bar{\ell}_A, \mathbf{b}_\tau]}{\int_{\mathcal{L}} \mu_1(d\bar{\ell}_A) \prod_{\tau=1}^t \mathbb{P}[\mathbf{i}_{\tau+1}^{(D)} | \bar{\ell}_A, \mathbf{b}_\tau]} \\ &= \frac{\mu_1(\bar{\ell}_A) \exp \left( \ln \left( \prod_{\tau=1}^t \frac{\mathbb{P}[\mathbf{i}_{\tau+1}^{(D)} | \bar{\ell}_A, \mathbf{b}_\tau]}{\mathbb{P}[\mathbf{i}_{\tau+1}^{(D)} | \ell_A, \mathbf{b}_\tau]} \right) \right)}{\int_{\mathcal{L}} \mu_1(d\bar{\ell}_A) \exp \left( \ln \left( \prod_{\tau=1}^t \frac{\mathbb{P}[\mathbf{i}_{\tau+1}^{(D)} | \bar{\ell}_A, \mathbf{b}_\tau]}{\mathbb{P}[\mathbf{i}_{\tau+1}^{(D)} | \ell_A, \mathbf{b}_\tau]} \right) \right)} \\ &= \frac{\mu_1(\bar{\ell}_A) \exp(-tZ_{t+1}(\bar{\ell}_A))}{\int_{\mathcal{L}} \mu_1(d\bar{\ell}_A) \exp(-tZ_{t+1}(\bar{\ell}_A))}, \end{aligned} \quad (27)$$

where  $Z_t$  is defined in Lemma 7. Step (a) above is well-defined by Assumption 1 and follows because  $\mathbf{I}^{(D)}$  is conditionally independent of  $\mathbf{h}_{t-1}^{(D)}$  given  $\mathbf{b}_{t-1}$ .

Using the expression in (27), we obtain that

$$\begin{aligned} \mathbb{E}_{\bar{\ell}_A \sim \mu_{t+1}} \left[ \overbrace{K(\bar{\ell}_A, \nu_t) - K_{\mathcal{L}}^*(\nu_t)}^{\triangleq \Delta K(\bar{\ell}_A, \nu_t)} \right] & \quad (28) \\ &= \frac{\int_{\mathcal{L}} \Delta K(\bar{\ell}_A, \nu_t) \mu_1(d\bar{\ell}_A) \exp(-tZ_{t+1}(\bar{\ell}_A))}{\int_{\mathcal{L}} \mu_1(d\bar{\ell}_A) \exp(-tZ_{t+1}(\bar{\ell}_A))} \\ &= \frac{\overbrace{\int_{\mathcal{L}} \Delta K(\bar{\ell}_A, \nu_t) \mu_1(d\bar{\ell}_A) \exp(-t(Z_{t+1}(\bar{\ell}_A) - K_{\mathcal{L}}^*(\nu_{t+1})))}^{\triangleq \sigma}}{\int_{\mathcal{L}} \mu_1(d\bar{\ell}_A) \exp(-t(Z_{t+1}(\bar{\ell}_A) - K_{\mathcal{L}}^*(\nu_{t+1})))}. \end{aligned}$$

By defining  $\mathcal{L}_\epsilon \triangleq \{\bar{\ell}_A | \Delta K(\bar{\ell}_A, \nu_{t+1}) \geq \epsilon\}$  we can write the numerator in (28) as

$$\int_{\mathcal{L} \setminus \mathcal{L}_\epsilon} \sigma + \int_{\mathcal{L}_\epsilon} \sigma \leq \epsilon + \int_{\mathcal{L} \setminus \mathcal{L}_\epsilon} \sigma. \quad (29)$$

Given this bound, it suffices to show that, for arbitrarily small  $\epsilon > 0$ ,

$$\lim_{t \rightarrow \infty} \frac{\int_{\mathcal{L}_\epsilon} \sigma}{\int_{\mathcal{L}} \mu_1(d\bar{\ell}_A) \exp(-t(Z_{t+1}(\bar{\ell}_A) - K_{\mathcal{L}}^*(\nu_{t+1})))} = 0.$$

Towards the proof of the limit above, we note that the exponent in  $\sigma$  (28) can be written as

$$\begin{aligned} & -t(Z_{t+1}(\bar{\ell}_A) - K_{\mathcal{L}}^*(\nu_{t+1})) \\ &= -t(Z_{t+1}(\bar{\ell}_A) - K_{\mathcal{L}}^*(\nu_{t+1})) + K(\bar{\ell}_A, \nu_{t+1}) - K(\bar{\ell}_A, \nu_{t+1}) \\ &= -t(\Delta K(\bar{\ell}_A, \nu_{t+1}) + Z_{t+1}(\bar{\ell}_A) - K(\bar{\ell}_A, \nu_{t+1})). \end{aligned} \quad (30)$$

Next, we recall from Lemma 7 that for any  $\epsilon > 0$ , there exists  $\eta > 0$  and  $t_\eta \geq 1$  such that, for all  $t \geq t_\eta$  and  $\bar{\ell}_A \in \mathcal{L}$ ,  $|Z_t(\bar{\ell}_A - K(\bar{\ell}_A, \nu_{t+1}))| < \eta$ . ( $t_\eta$  is uniform as  $|\mathcal{L}| < \infty$ , Assumption 1.) This fact together with (30) implies that

$$\begin{aligned} & \frac{\int_{\mathcal{L}_\epsilon} \Delta K(\bar{\ell}_A, \nu_{t+1}) \mu_1(d\bar{\ell}_A) \exp(-t(Z_{t+1}(\bar{\ell}_A) - K_{\mathcal{L}}^*(\nu_{t+1})))}{\int_{\mathcal{L}} \mu_1(d\bar{\ell}_A) \exp(-t(Z_{t+1}(\bar{\ell}_A) - K_{\mathcal{L}}^*(\nu_{t+1})))} \\ & \leq \frac{\int_{\mathcal{L}_\epsilon} \Delta K(\bar{\ell}_A, \nu_{t+1}) \mu_1(d\bar{\ell}_A) \exp(-t(\Delta K(\bar{\ell}_A, \nu_{t+1}) - \eta))}{\int_{\mathcal{L}} \mu_1(d\bar{\ell}_A) \exp(-t(\Delta K(\bar{\ell}_A, \nu_{t+1}) + \eta))} \\ & = e^{2t\eta} \frac{\int_{\mathcal{L}_\epsilon} \Delta K(\bar{\ell}_A, \nu_{t+1}) \mu_1(d\bar{\ell}_A) e^{-t\Delta K(\bar{\ell}_A, \nu_{t+1})}}{\int_{\mathcal{L}} \mu_1(d\bar{\ell}_A) e^{-t\Delta K(\bar{\ell}_A, \nu_{t+1})}} \end{aligned} \quad (*)$$

for all  $t \geq t_\eta$ .

Now consider the numerator in (\*). Since  $x e^{-tx}$  is decreasing for all  $x > t^{-1}$  and since  $\Delta K(\bar{\ell}_A, \nu_{t+1}) \geq \epsilon$  for all  $\bar{\ell}_A \in \mathcal{L}_\epsilon$ , we have that

$$\int_{\mathcal{L}_\epsilon} \Delta K(\bar{\ell}_A, \nu_{t+1}) \mu_1(d\bar{\ell}_A) e^{-t\Delta K(\bar{\ell}_A, \nu_{t+1})} \leq \epsilon e^{-t\epsilon}$$

for any  $t \geq \max[t_\eta, \frac{1}{\epsilon}]$ .

Next consider the denominator in (\*). By definition,  $\exists \bar{\ell}_A \in \mathcal{L}$  such that  $K(\bar{\ell}_A, \nu_t) = K_{\mathcal{L}}^*(\nu_t) \forall t$ . This fact together with the assumption that  $\mu_1$  has full support (Assumption 1) means that the denominator is a positive constant, which we denote by  $k$ . As a consequence, (\*)  $\leq e^{2t\eta} \epsilon e^{-t\epsilon} k^{-1}$ . Let  $\eta = \frac{\epsilon}{4}$ . Then  $e^{2t\eta} \epsilon e^{-t\epsilon} k^{-1} = e^{-\frac{t\epsilon}{2}} \epsilon k^{-1}$ , which converges to 0 as  $t \rightarrow \infty$ . Consequently,  $\lim_{t \rightarrow \infty} \mathbb{E}_{\bar{\ell}_A \sim \mu_t} [\Delta K(\bar{\ell}_A, \nu_t)] = 0$  a.s.- $\mathbb{P}^{\mathcal{L}}$ .

APPENDIX D  
PROOF OF THEOREM 4.B

The proof of Thm. 4.B follows the same procedure as that of Thm. 4.A, with the difference that  $\Theta_k$  is allowed to be non-finite, whereas  $\mathcal{L}$  in Thm. 4.A is finite (Assumption 1).

Define  $\Theta_{k,\epsilon}^+ \triangleq \{\bar{\theta} | \Delta K(\bar{\theta}, \nu_t) \geq \epsilon\}$  and  $\Theta_{k,\frac{\epsilon}{2}}^- \triangleq \{\bar{\theta} | \Delta K(\bar{\theta}, \nu_t) \leq \frac{\epsilon}{2}\}$ . It then follows from (29) that

$$\int_{\Theta_k} \underbrace{\left( K(\bar{\theta}, \nu_t) - K_{\Theta_k}^*(\nu_t) \right)}_{\Delta K(\bar{\theta}, \nu_t)} \rho_t^{(k)}(d\bar{\theta}) \leq \epsilon + \underbrace{\frac{\int_{\Theta_{k,\epsilon}^+} \Delta K(\bar{\theta}, \nu_t) \exp(-t(Z_t(\bar{\theta}) - K_{\Theta_k}^*(\nu_t))) \rho_1^{(k)}(d\bar{\theta})}{\int_{\Theta_{k,\frac{\epsilon}{2}}^-} \exp(-t(Z_t(\bar{\theta}) - K_{\Theta_k}^*(\nu_t))) \rho_1^{(k)}(d\bar{\theta})}}_{\triangleq \star}, \quad (31)$$

where  $\star$  is well-defined by Assumptions 1–2.

(31) implies that it suffices to prove that  $\star \xrightarrow{t \rightarrow \infty} 0$  for arbitrarily small  $\epsilon$ . Applying Lemma 7 and (\*), we obtain

$$\begin{aligned} \star &\stackrel{(a)}{\leq} e^{2t\eta} \frac{\int_{\Theta_{k,\epsilon}^+} \Delta K(\bar{\theta}, \nu_t) e^{-t\Delta K(\bar{\theta}, \nu_t)} \rho_1^{(k)}(d\bar{\theta})}{\int_{\Theta_{k,\frac{\epsilon}{2}}^-} e^{-t\Delta K(\bar{\theta}, \nu_t)} \rho_1^{(k)}(d\bar{\theta})} \\ &\stackrel{(b)}{\leq} e^{2t\eta} \frac{\epsilon e^{-t\epsilon}}{\int_{\Theta_{k,\frac{\epsilon}{2}}^-} e^{-t\Delta K(\bar{\theta}, \nu_t)} \rho_1^{(k)}(d\bar{\theta})} \\ &\stackrel{(c)}{\leq} e^{2t\eta} \frac{\epsilon e^{-t\epsilon}}{e^{-t\frac{\epsilon}{2}} \int_{\Theta_{k,\frac{\epsilon}{2}}^-} \rho_1^{(k)}(d\bar{\theta})} = e^{2t\eta} \frac{\epsilon e^{-t\frac{\epsilon}{2}}}{\rho_1^{(k)}(\Theta_{k,\frac{\epsilon}{2}}^-)} \end{aligned}$$

for all  $t \geq \max[t_\eta, \epsilon^{-1}]$ , where (a) follows from (\*); (b) follows because  $x e^{-tx}$  is decreasing for all  $x > t^{-1}$ ; and (c) follows because  $e^{-t\Delta K(\bar{\theta}, \nu_t)} \geq e^{-t\frac{\epsilon}{2}}$ .

Let  $\eta = \epsilon/8$ . Then the numerator in the final expression above becomes  $\epsilon e^{-t\frac{\epsilon}{4}}$ , which converges to 0 as  $t \rightarrow \infty$ . Thus what remains to show is that the denominator is positive in the limit, i.e.,  $\lim_{t \rightarrow \infty} \rho_1^{(k)}(\Theta_{k,\frac{\epsilon}{2}}^-) > 0$ . We prove this statement by establishing uniform continuity of  $\Delta K(\bar{\theta}, \nu)$ . Towards this end, we prove the following two lemmas.

**Lemma 8.**  $\mathcal{B}$  (5) is a compact subset of  $\mathbb{R}^{|\mathcal{S}|}$  with the Euclidean metric  $d$  and  $\Delta(\mathcal{B})$  a compact metric space with the Wasserstein- $p$  distance  $W_p$  ( $p \geq 1$ ).

*Proof.* Since  $\mathcal{S}$  is finite,  $\mathcal{B} = \Delta(\mathcal{S})$  is a compact subset of  $\mathbb{R}^{|\mathcal{S}|}$ . To prove that  $(\Delta(\mathcal{B}), W_p)$  is compact we will show that every sequence  $(\nu_n)_{n=1}^\infty \subset \Delta(\mathcal{B})$  admits a subsequence converging to some limit point in  $\Delta(\mathcal{B})$ . This collection of measures is tight as  $\exists C \subseteq \mathcal{B}$  such that  $\nu_n(C) = 1 > 1 - \epsilon$  for any  $\epsilon > 0$  and  $\nu_n$ . As a consequence,  $(\nu_n)_{n=1}^\infty$  admits a limit point  $\nu^* \in \Delta(\mathcal{B})$  w.r.t the topology of weak convergence (Prokhorov's theorem [83, Ch. 1,§5]).

We will show that  $\nu^*$  is also a limit point under  $W_p$ . By Skorokhod's representation theorem [83, pp. 70], there exists a sequence of  $\mathcal{B}$ -valued random variables  $\{V_1, \dots, V_n, \dots, V^*\}$  such that  $V_n$  has the probability law  $\nu_n$  and  $\lim_{n \rightarrow \infty} d(V_n, V^*) = 0$  almost surely. By the dominance convergence theorem and the facts that  $\mathcal{B}$  is compact and  $d$

is continuous,  $\lim_{n \rightarrow \infty} \mathbb{E}[d(V_n, V^*)^p] = 0$ . Consequently, for any coupling  $\xi$  between  $\nu_n$  and  $\nu^*$ ,

$$\lim_{n \rightarrow \infty} \left( \int d(x, y)^p d\xi(x, y) \right)^{\frac{1}{p}} = 0.$$

Since  $W_p(\nu_n, \nu^*)$  is the infimum of the left-hand side above,  $\lim_{n \rightarrow \infty} W_p(\nu_n, \nu^*) = 0$ . Hence  $(\Delta(\mathcal{B}), W_p)$  is compact.  $\square$

**Lemma 9.**  $\Delta K(\bar{\theta}, \nu) \triangleq K(\bar{\theta}, \nu) - K_{\Theta_k}^*(\nu)$  is a continuous map from  $(\Theta_k, d) \times (\Delta(\mathcal{B}), W_1)$  to  $\mathbb{R}$ , where  $d$  and  $W_1$  denote the Euclidean and the Wasserstein-1 distance, respectively.

*Proof.* We start by showing that  $K(\bar{\theta}, \nu)$  is continuous by proving that for any convergent sequence  $(\bar{\theta}_n, \nu_n) \xrightarrow{n \rightarrow \infty} (\bar{\theta}, \nu)$ , the difference  $|K(\bar{\theta}_n, \nu_n) - K(\bar{\theta}, \nu)|$  converges to 0. This difference can be bounded as

$$\begin{aligned} |K(\bar{\theta}_n, \nu_n) - K(\bar{\theta}, \nu)| &\leq \underbrace{|K(\bar{\theta}_n, \nu_n) - K(\bar{\theta}_n, \nu)|}_{\triangleq \textcircled{1}} + \underbrace{|K(\bar{\theta}_n, \nu) - K(\bar{\theta}, \nu)|}_{\triangleq \textcircled{2}}. \end{aligned}$$

Consider the left expression above (①). (17) implies that

$$\begin{aligned} \textcircled{1} &= \left| \int_{\mathcal{B}} \mathbb{E}_{\mathbf{I}^{(k)}} \left[ \ln \left( \frac{\mathbb{P}[\mathbf{I}^{(k)} | \boldsymbol{\theta}, \mathbf{b}]}{\mathbb{P}[\mathbf{I}^{(k)} | \bar{\boldsymbol{\theta}}_n, \mathbf{b}]} \right) \right] \nu_n(d\mathbf{b}) \right. \\ &\quad \left. - \int_{\mathcal{B}} \mathbb{E}_{\mathbf{I}^{(k)}} \left[ \ln \left( \frac{\mathbb{P}[\mathbf{I}^{(k)} | \boldsymbol{\theta}, \mathbf{b}]}{\mathbb{P}[\mathbf{I}^{(k)} | \bar{\boldsymbol{\theta}}_n, \mathbf{b}]} \right) \right] \nu(d\mathbf{b}) \right|, \end{aligned}$$

which is an integral probability metric (IPM) with the testing function  $f(b) \triangleq \mathbb{E}_{\mathbf{I}^{(k)}} \left[ \ln \left( \frac{\mathbb{P}[\mathbf{I}^{(k)} | \boldsymbol{\theta}, \mathbf{b}]}{\mathbb{P}[\mathbf{I}^{(k)} | \bar{\boldsymbol{\theta}}_n, \mathbf{b}]} \right) \right]$ . This function is assumed to be Lipschitz continuous (Assumption 2.1). Without loss of generality, we assume that the Lipschitz constant is 1. Since the Wasserstein distance is equivalent to the IPM w.r.t the class of 1-Lipschitz functions, ① is upper-bounded by  $W_p(\nu_n, \nu)$ . Hence, as  $\nu_n$  converges to  $\nu$  in  $W_p$ , ① converges to 0.

We now show that ② converges. Using Assumption 2.2 and the dominated convergence theorem, we obtain that

$$\begin{aligned} \lim_{n \rightarrow \infty} \mathbb{E}_{\mathbf{b} \sim \nu} \mathbb{E}_{\mathbf{I}^{(k)}} \left[ \ln \left( \frac{\mathbb{P}[\mathbf{I}^{(k)} | \boldsymbol{\theta}, \mathbf{b}]}{\mathbb{P}[\mathbf{I}^{(k)} | \bar{\boldsymbol{\theta}}_n, \mathbf{b}]} \right) \right] \\ = \mathbb{E}_{\mathbf{b} \sim \nu} \mathbb{E}_{\mathbf{I}^{(k)}} \left[ \ln \left( \frac{\mathbb{P}[\mathbf{I}^{(k)} | \boldsymbol{\theta}, \mathbf{b}]}{\mathbb{P}[\mathbf{I}^{(k)} | \bar{\boldsymbol{\theta}}, \mathbf{b}]} \right) \right], \end{aligned}$$

which implies that  $\bar{\theta} \mapsto K(\bar{\theta}, \nu)$  is continuous and that ② converges to 0 as  $n \rightarrow \infty$ .

Finally, applying Berge's maximum theorem [84, Thm. 17.31] to  $K(\bar{\theta}, \nu)$  w.r.t.  $\bar{\theta}$  yields that the mapping  $\nu \mapsto K_{\Theta_k}^*(\nu)$  is continuous, which implies continuity of  $\Delta K$ .  $\square$

#### A. Proof of Theorem 4.B

Lemmas 8–9 imply uniform continuity of  $\Delta K(\bar{\theta}, \nu)$  and Berge's maximum theorem implies that  $|\Theta_k^*(\nu)| > 0$  [84, Thm. 17.31]. Therefore,  $\exists \delta_m$  such that  $d(\bar{\theta}_\nu, \bar{\theta}') < \delta_m$  and  $W_1(\nu, \nu') < \delta_m$ . This means that  $\Delta K(\bar{\theta}', \nu') \leq \Delta K(\bar{\theta}_\nu, \nu) + m = m$ , where the last equality follows because  $\bar{\theta}_\nu \in$

$\Theta_k^*(\nu) \implies \Delta K(\bar{\theta}_\nu, \nu) = 0$ . As a consequence, for any  $\nu \in \Delta(\mathcal{B})$  and  $\nu' \in B(\nu, \delta_m) \triangleq \{\nu' | W_1(\nu, \nu') < \delta_m\}$ ,

$$\underbrace{\{\bar{\theta}' | d(\bar{\theta}', \bar{\theta}_\nu) < \delta_m\}}_{\Theta_{\nu}(\delta_m)} \subset \underbrace{\{\bar{\theta}' | \Delta K(\bar{\theta}', \nu) \leq m\}}_{\Theta_{\nu'}(m)}.$$

Thus, for any  $\nu$  and  $\nu' \in B(\nu, \delta_m)$ ,

$$\rho_1^{(k)}(\Theta_{\nu'}(m)) \geq \rho_1^{(k)}(\Theta_{\nu}(\delta_m)) > 0,$$

where the strict inequality follows because  $\rho_1^{(k)}$  has full support (Assumption 1).

The set  $\{B(\nu, \delta_m)\}_{\nu \in \Delta(\mathcal{B})}$  forms an open cover for a compact space, which means that there exists a finite sub-cover  $\{B(\nu_i, \delta_m)\}_{i=1}^M$ . As a consequence,  $\nu' \in \Delta(\mathcal{B})$  belongs to some Wasserstein ball  $B(\nu_i, \delta_m)$ . Let  $r \triangleq \min_i \rho_1^{(k)}(\Theta_{\nu_i}(\delta_m)) > 0$ . We then have that

$$\rho_1^{(k)}(\Theta_{\nu'}(m)) \geq \rho_1^{(k)}(\Theta_{\nu_i}(\delta_m)) \geq r,$$

which yields  $\rho_1^{(k)}(\Theta_{k, \frac{\epsilon}{2}}^-) \geq r > 0$  with  $m = \frac{\epsilon}{2}$ .  $\square$

## APPENDIX E

### EXAMPLE DERIVATION OF A BERK-NASH EQUILIBRIUM

We use the following example to illustrate the steps required to find a Berk-Nash equilibrium.

**Example 1.** Consider Prob. 1 with  $N = 1$ ,  $p_A = 1$ ,  $\mathcal{O} = \{0, 1\}$ ,  $z_{\theta_i}(\cdot|0) = \text{Ber}(p)$ ,  $z_{\theta_i}(1|1) = \text{Ber}(q)$ , and  $c$  being defined as in Fig. 3. Let the rollout parameters be  $(\ell_A = 0, \ell_D = 1)$  and let  $\pi_1$  be threshold strategies with  $\beta \geq 0$  and  $\alpha \leq 1$  (Thm. 1). Finally, let  $\mathcal{L} = \{\ell_A\}$ ,  $\Theta_A = \{\theta_1\}$ , and  $\Theta_D = \{\bar{\theta}_a, \bar{\theta}_b\}$ , where  $z_{\bar{\theta}_a}(0|0) = z_{\bar{\theta}_a}(1|1) = z_{\bar{\theta}_b}(1|0) = z_{\bar{\theta}_b}(0|1) = 1$ .

We start with condition (i) in Def. 2. Since  $\ell_A = 0$ , it suffices to consider  $\pi_D$ . By the principle of optimality

$$\pi_D(b) \in \arg \min_{a \in \mathcal{A}_D} \mathbb{E}_{S, B'} \left[ c(S, a) + \gamma \bar{J}_{D, \bar{\theta}}^{(\pi_1)}(B') \mid b, \pi_1 \right],$$

where  $\bar{J}_{D, \bar{\theta}}^{(\pi_1)}(B') = (1 - \gamma \mathbf{P}_{\bar{\theta}_a, \pi_1})^{-1} \mathbf{c}_{\pi_1}$ . From the definition of  $\Theta_D$  we obtain that  $b = \mathbb{P}[S = 1] \in \{0, 1\}$  and that

$$\mathbf{P}_{\bar{\theta}_a, \pi_1} = \begin{bmatrix} 1 - q & q \\ 1 & 0 \end{bmatrix}, \quad \mathbf{P}_{\bar{\theta}_b, \pi_1} = \begin{bmatrix} 1 - p & p \\ 1 & 0 \end{bmatrix}, \quad \mathbf{c}_{\pi_1} = \begin{bmatrix} 0 \\ -1 \end{bmatrix}.$$

Simple algebra yields

$$\bar{J}_{D, \bar{\theta}_a}^{(\pi_1)} = \frac{1}{(\gamma - 1)(1 + \gamma q)} \left[ 1 + \gamma(q - 1) \right],$$

where  $q$  is exchanged for  $p$  when the conjecture is  $\bar{\theta}_b$ . Hence, to meet condition (i), the defender's rollout strategy must satisfy  $\pi_D(0) = C$  and  $\pi_D(1) = S$ , which is ensured by (13). As a consequence,  $\pi = \pi_1$  in any Berk-Nash equilibrium.

Now consider condition (ii); (17) can be written as

$$\begin{aligned} K(\bar{\theta}, \nu) &= \mathbb{E}_{b \sim \nu} \mathbb{E}_{\mathbf{I}^{(D)}} \left[ \ln \left( \frac{\mathbb{P}[\mathbf{I}^{(D)} \mid \theta, b]}{\mathbb{P}[\mathbf{I}^{(D)} \mid \bar{\theta}, b]} \right) \mid \theta, b \right] \\ &= - \sum_{b \in \{0, 1\}} \nu(b) \sum_{o \in \{0, 1\}} z_{\theta}(o \mid b) \ln z_{\bar{\theta}}(o \mid b) + \text{const.} \end{aligned}$$

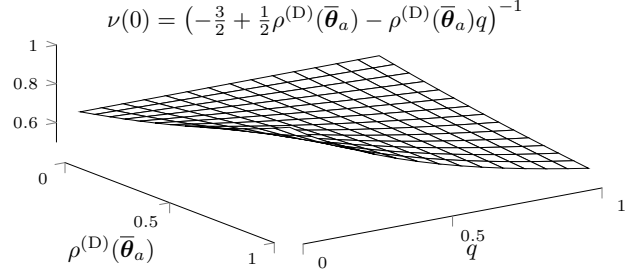


Fig. 15: Berk-Nash equilibria of Example 1 when  $p = \frac{1}{2}$ .

Minimizing the above expression with respect to  $\bar{\theta}$  yields  $\Theta_D^* = \{\bar{\theta}_a\}$  if  $(p = 0, q = 1)$ ,  $\Theta_D^* = \{\bar{\theta}_b\}$  if  $(p = 1, q = 0)$ , and  $\Theta_D^*(\nu) = \{\bar{\theta}_a, \bar{\theta}_b\}$  otherwise.

Lastly, condition (iii) is satisfied iff  $\mathbf{P}_{\bar{\theta}, \pi_1}^T \nu = \nu$ . Solving this equation yields

$$\nu(0) = - \left( -1 - p + \rho^{(D)}(\bar{\theta}_a)p - \rho^{(D)}(\bar{\theta}_a)q \right)^{-1}, \quad (32)$$

which means the Berk-Nash equilibrium is not unique and may not exist (see Fig. 15). For example, if  $p = 1$  and  $q = 0$ , then (32) requires that  $\rho^{(D)}(\bar{\theta}_a) = 1$ , but this means that  $\rho^{(D)} \notin \Delta(\Theta^*(\nu))$ , which violates condition (ii).

## APPENDIX F

### HYPERPARAMETERS

The hyperparameters used for the evaluation in this paper are listed in Table 5 and were obtained through grid search.

## APPENDIX G

### CONFIGURATION OF THE INFRASTRUCTURE IN FIG. 1

The configuration of the target infrastructure (Fig. 1) is available in Table 6.

## REFERENCES

- [1] M. H. Manshaei, Q. Zhu, T. Alpcan, T. Basar, and J.-P. Hubaux, "Game theory meets network security and privacy," *ACM Comput. Surv.*, vol. 45, no. 3, pp. 25:1–25:39, Jul. 2013.
- [2] M. van Dijk, A. Juels, A. Oprea, and R. L. Rivest, "Flipit: The game of "stealthy takeover,"" *Journal of Cryptology*, no. 4, Oct 2013.
- [3] L. Huang and Q. Zhu, "A dynamic games approach to proactive defense strategies against advanced persistent threats in cyber-physical systems," *Computers & Security*, vol. 89, p. 101660, 11 2019.
- [4] T. Li, Y. Zhao, and Q. Zhu, "The role of information structures in game-theoretic multi-agent learning," *Annual Reviews in Control*, vol. 53, pp. 296–314, 2022.
- [5] C. Kamhoua, C. Kiekintveld, F. Fang, and Q. Zhu, *Game Theory and Machine Learning for Cyber Security*. Wiley, 2021.
- [6] K. Durkota, V. Lisy, B. Bošanský, and C. Kiekintveld, "Optimal network security hardening using attack graph games," in *Proceedings of the 24th International Conference on Artificial Intelligence*, 2015.
- [7] K. Horák, B. Bosanský, P. Tomásek, C. Kiekintveld, and C. A. Kamhoua, "Optimizing honeypot strategies against dynamic lateral movement using partially observable stochastic games," *Comput. Secur.*, vol. 87, 2019.
- [8] K. Hammar and R. Stadler, "Learning near-optimal intrusion responses against dynamic attackers," *IEEE Transactions on Network and Service Management*, pp. 1–1, 2023.
- [9] —, "Scalable learning of intrusion response through recursive decomposition," in *Decision and Game Theory for Security*, J. Fu, T. Kroupa, and Y. Hayel, Eds. Cham: Springer Nature Switzerland, 2023, pp. 172–192.

Figures and Tables	Values
Fig. 6	$\mathcal{O} = \{0, \dots, 9\}$ , $p_A = 0.1, \gamma = 0.99$ , $z(\cdot   0) = \text{BetaBin}(n = 10, \alpha = 0.7, \beta = 3)$ , $z(\cdot   1) = \text{BetaBin}(n = 10, \alpha = 1, \beta = 0.7)$
Fig. 5	$\mathcal{O} = \{0, \dots, 9\}$ , $p_A = 0.1, N = 1, \gamma = 0.99$ $z(\cdot   0) = \text{BetaBin}(n = 10, \alpha = 0.7, \beta = 3)$ , $z(\cdot   1) = \text{BetaBin}(n = 10, \alpha = 1, \beta = 0.7)$
Fig. 9	$N = 10, p_A = 0.1, \gamma = 0.99$ $\pi_{D,1}(\mathcal{S}   \mathbf{b}_t) = 1 \iff \mathbb{P}[S_t \geq 1   \mathbf{b}_t] \geq 0.75$ $\pi_{A,1}(\mathcal{S}   \mathbf{b}_t, s_t) = 0.5$ Cost function of base strategy estimated using 100 MC samples w. horizon 50
Figs. 13.a-e	$\ell_A = \ell_D = 1, \mathcal{L} = \{1, 2\}, p_A = 1$ $\pi_{D,1}(\mathcal{S}   \mathbf{b}_t) = 1 \iff \mathbb{P}[S_t \geq 1   \mathbf{b}_t] \geq 0.75$ $\pi_{A,1}(\mathcal{S}   \mathbf{b}_t, s_t) = 0.05$ $N = 10, \mathcal{O}, z$ (Fig. 12) using 100 MC samples w. horizon 50
Fig. 4, Fig. 13.f	$\mathcal{O}, z$ (Fig. 12), $p_A = 0.1, \gamma = 0.99$ , $\mathcal{L} = 0, 1, 2, N = 10$ $\pi_{D,1}(\mathcal{S}   \mathbf{b}_t) = 1 \iff \mathbb{P}[S_t \geq 1   \mathbf{b}_t] \geq 0.75$ $\pi_{A,1}(\mathcal{S}   \mathbf{b}_t, s_t) = 0.05$ Best response computation: CEM [39] Best responses parameterized following Thm. 1
Figs. 13.g-o, 14	$\ell_A = \ell_D = 1, p_A = 1, \gamma = 0.99$ $\pi_{D,1}(\mathcal{S}   \mathbf{b}_t) = 1 \iff \mathbb{P}[S_t \geq 1   \mathbf{b}_t] \geq 0.75$ $\pi_{A,1}(\mathcal{S}   \mathbf{b}_t, s_t) = 0.05$ $N = 10, \mathcal{O}, z$ (Fig. 12) using 100 MC samples w. horizon 50
Fig. 13.k Table 3	$\Theta_D = \{0, \dots, 200\}$ $\ell_A = \ell_D = 1, p_A = 1, \gamma = 0.99$ $\pi_{D,1}(\mathcal{S}   \mathbf{b}_t) = 1 \iff \mathbb{P}[S_t \geq 1   \mathbf{b}_t] \geq 0.75$ $\pi_{A,1}(\mathcal{S}   \mathbf{b}_t, s_t) = 0.05$ $N = 10, \mathcal{O}, z$ (Fig. 12, $t = 10$ ) using 100 MC samples w. horizon 50
Fig. 11	$\psi = (\frac{1}{2}, 10^{-2}, -10^5)$ , $\chi = (1.0593)$ , $\phi = (-0.5193)$ , $\omega = (0.054\pi)$ , time-step: 30s, service time: $\text{Exp}(\mu = 4)t$ , computed using the Student-t distribution
Confidence intervals	Approximate threshold best responses against randomized opponents (Fig. 4)
Base strategies $\pi_{D,1} \pi_{A,1}$	uniform
Priors $\mu_1, \rho_1^{(D)}, \rho_1^{(A)}$	$p = 5/4, q = 1, r = 2$
Cost function (7), Fig. 3	
HSV1 Parameter	
$\epsilon$	0.1
<b>Cross-entropy method [39]</b>	
$\lambda$ (fraction of samples to keep)	0.15, 100
$K$ population size	100
$M$ number of samples for each evaluation	50
<b>PPO [59, Alg. 1] parameters</b>	
lr $\alpha$ , batch, # layers, # neurons, clip $\epsilon$	$10^{-5}, 4 \cdot 10^3 t, 4, 64, 0.2$ ,
GAE $\lambda$ , ent-coef, activation	$0.95, 10^{-4}, \text{ReLU}$
<b>NFSP [60, Alg. 9] parameters</b>	
lr RL, lr SL, batch, # layers, # neurons, $\mathcal{M}_{RL}$	$10^{-2}, 5 \cdot 10^{-3}, 64, 2, 128, 2 \times 10^5$
$\mathcal{M}_{SL}, \epsilon, \epsilon$ -decay, $\eta$	$2 \times 10^6, 0.06, 0.001, 0.1$

TABLE 5: Hyperparameters.

[10] Y. Zhao, L. Huang, C. Smidts, and Q. Zhu, "Finite-horizon semi-markov game for time-sensitive attack response and probabilistic risk assessment in nuclear power plants," *Reliability Engineering & System Safety*, vol. 201, p. 106878, 2020.

[11] J. Chen and Q. Zhu, "Interdependent strategic security risk management with bounded rationality in the internet of things," *IEEE Transactions on Information Forensics and Security*, vol. 14, no. 11, pp. 2958–2971, 2019.

[12] D. Bertsekas, *Rollout, Policy Iteration, and Distributed Reinforcement Learning*, ser. Athena scientific optimization and computation series. Athena Scientific, 2021.

[13] I. Esponda and D. Pouzo, "Berk-nash equilibrium: A framework for modeling agents with misspecified models," *Econometrica*, vol. 84, no. 3, pp. 1093–1130, 2023/10/13/ 2016.

[14] J. H. Kagel and D. Levin, "The winner's curse and public information in common value auctions," *The American Economic Review*, vol. 76, no. 5, pp. 894–920, 1986.

[15] M. Rabin, "Inference by believers in the law of small numbers," *The Quarterly Journal of Economics*, vol. 117, no. 3, pp. 775–816, 2002.

[16] H. A. Simon, "Theories of bounded rationality," *Decision and Organization*, pp. 161–176, 1972.

[17] L. Samuelson, "Bounded rationality and game theory," *The Quarterly Review of Economics and Finance*, vol. 36, no. Supplemen, pp. 17–35, 1996.

[18] R. W. Rosenthal, "A bounded-rationality approach to the study of noncooperative games," *International Journal of Game Theory*, vol. 18, no. 3, pp. 273–292, Sep 1989.

[19] A. Sanjab, W. Saad, and T. Başar, "A game of drones: Cyber-physical security of time-critical uav applications with cumulative prospect theory perceptions and valuations," *IEEE Transactions on Communications*, vol. 68, no. 11, pp. 6990–7006, 2020.

[20] R. Gabrys, M. Bilinski, J. Mauger, D. Silva, and S. Fugate, "Casino rationale: Countering attacker deception in zero-sum stackelberg security games of bounded rationality," in *Decision and Game Theory for Security*, F. Fang, H. Xu, and Y. Hayel, Eds. Cham: Springer International Publishing, 2023, pp. 23–43.

[21] J. Chen and Q. Zhu, "Security investment under cognitive constraints: A gestalt nash equilibrium approach," in *2018 52nd Annual Conference on Information Sciences and Systems (CISS)*, 2018, pp. 1–6.

[22] A. Sinha, F. Fang, B. An, C. Kiekintveld, and M. Tambe, "Stackelberg security games: Looking beyond a decade of success," in *Proceedings of the Twenty-Seventh International Joint Conference on Artificial Intelligence, IJCAI-18*. International Joint Conferences on Artificial Intelligence Organization, 7 2018, pp. 5494–5501.

[23] Z. Wan, J.-H. Cho, M. Zhu, A. H. Anwar, C. A. Kamhoua, and M. P. Singh, "Four-eye: Defensive deception against advanced persistent threats via hypergame theory," *IEEE Transactions on Network and Service Management*, vol. 19, no. 1, pp. 112–129, 2022.

[24] C. Bakker, A. Bhattacharya, S. Chatterjee, and D. L. Vrabie, "Learning and information manipulation: Repeated hypergames for cyber-physical security," *IEEE Control Systems Letters*, vol. 4, no. 2, pp. 295–300, 2020.

[25] M. Abdallah, P. Naghizadeh, A. R. Hota, T. Cason, S. Bagchi, and S. Sundaram, "Behavioral and game-theoretic security investments in interdependent systems modeled by attack graphs," *IEEE Transactions on Control of Network Systems*, vol. 7, no. 4, pp. 1585–1596, 2020.

[26] C. N. Mavridis, A. Kanellopoulos, K. G. Vamvoudakis, J. S. Baras, and K. H. Johansson, "Attack identification for cyber-physical security in dynamic games under cognitive hierarchy," *IFAC-PapersOnLine*, vol. 56, no. 2, pp. 11 223–11 228, 2023, 22nd IFAC World Congress.

[27] D. Fudenberg and D. K. Levine, *The theory of learning in games*. MIT Press, Cambridge, MA, 1998.

[28] H. P. Young, *Strategic learning and its limits*. Oxford University Press, 2004, cited by 0313.

[29] J. Hu and M. P. Wellman, "Nash q-learning for general-sum stochastic games," *J. Mach. Learn. Res.*, vol. 4, no. null, p. 1039–1069, dec 2003.

[30] M. L. Littman, "Markov games as a framework for multi-agent reinforcement learning," in *Proceedings of the Eleventh International Conference on Machine Learning*, ser. ICML'94. San Francisco, CA, USA: Morgan Kaufmann Publishers Inc., 1994, p. 157–163.

[31] Y. Ge, T. Li, and Q. Zhu, "Scenario-agnostic zero-trust defense with explainable threshold policy: A meta-learning approach," *IEEE INFOCOM 2023 - IEEE Conference on Computer Communications Workshops (INFOCOM WKSHPS)*, pp. 1–6, 2023.

[32] K. Hammar and R. Stadler, "Finding effective security strategies through reinforcement learning and Self-Play," in *International Conference on Network and Service Management (CNSM 2020)*, Izmir, Turkey, 2020.

[33] —, "Intrusion prevention through optimal stopping," *IEEE Transactions on Network and Service Management*, vol. 19, no. 3, pp. 2333–2348, 2022.

[34] CSLE, "Cyber security learning environment," 2023, documentation: <https://limmen.dev/csle/>, traces: <https://github.com/Limmen/csle/releases/tag/v0.4.0>, source code: <https://github.com/Limmen/csle>, video demonstration: <https://www.youtube.com/watch?v=IE2KpmtIs2A&>.

[35] K. Horák, B. Bošanský, V. Kovařík, and C. Kiekintveld, "Solving zero-sum one-sided partially observable stochastic games," *Artificial Intelligence*, vol. 316, p. 103838, 2023.

[36] J. Goldsmith and M. Mundhenk, "Competition adds complexity," in *Advances in Neural Information Processing Systems*, J. Platt, D. Koller, Y. Singer, and S. Roweis, Eds., vol. 20. Curran Associates, Inc., 2007.

[37] K. Horák, "Scalable algorithms for solving stochastic games with limited partial observability," Ph.D. dissertation, Czech Technical University in Prague, 2019.

[38] V. Krishnamurthy, *Partially Observed Markov Decision Processes: From Filtering to Controlled Sensing*. Cambridge University Press, 2016.

[39] R. Rubinstein, "The cross-entropy method for combinatorial and continuous optimization," *Methodology And Computing In Applied Probability*, vol. 1, no. 2, pp. 127–190, Sep 1999.

[40] J. F. Nash, "Non-cooperative games," *Annals of Mathematics*, vol. 54, pp. 286–295, 1951.

[41] J. von Neumann, "Zur Theorie der Gesellschaftsspiele. (German) [On the theory of games of strategy]," *j-MATH-ANN*, vol. 100, pp. 295–320, 1928.

[42] D. Fudenberg and J. Tirole, *Game Theory*. MIT Press, 1991.

[43] I.-K. Cho and D. M. Kreps, "Signaling games and stable equilibria," *The Quarterly Journal of Economics*, vol. 102, no. 2, pp. 179–221, 1987.

ID(s)	Type	Operating system	Zone	Services	Vulnerabilities
1	Gateway	UBUNTU 20	-	SNORT (ruleset v2.9.17.1), SSH, OPENFLOW v1.3, RYU SDN controller	-
2	Gateway	UBUNTU 20	DMZ	SNORT (ruleset v2.9.17.1), SSH, OVS v2.16, OPENFLOW v1.3	-
28	Gateway	UBUNTU 20	R&D	SNORT (ruleset v2.9.17.1), SSH, OVS v2.16, OPENFLOW v1.3	-
3,12	Switch	UBUNTU 22	DMZ	SSH, OPENFLOW v1.3, OVS v2.16	-
21,22	Switch	UBUNTU 22	-	SSH, OPENFLOW v1.3, OVS v2.16	-
23	Switch	UBUNTU 22	ADMIN	SSH, OPENFLOW v1.3, OVS v2.16	-
29-48	Switch	UBUNTU 22	R&D	SSH, OPENFLOW v1.3, OVS v2.16	-
13-16	Honeypot	UBUNTU 20	DMZ	SSH, SNMP, POSTGRES, NTP	-
17-20	Honeypot	UBUNTU 20	DMZ	SSH, IRC, SNMP, SSH, POSTGRES	-
4	App node	UBUNTU 20	DMZ	HTTP, DNS, SSH	CWE-1391
5, 6	App node	UBUNTU 20	DMZ	SSH, SNMP, POSTGRES, NTP	-
7	App node	UBUNTU 20	DMZ	HTTP, TELNET, SSH	CWE-1391
8	App node	DEBIAN JESSIE	DMZ	FTP, SSH, APACHE 2,SNMP	CVE-2015-3306
9,10	App node	UBUNTU 20	DMZ	NTP, IRC, SNMP, SSH, POSTGRES	-
11	App node	DEBIAN JESSIE	DMZ	APACHE 2, SMTP, SSH	CVE-2016-10033
24	Admin system	UBUNTU 20	ADMIN	HTTP, DNS, SSH	CWE-1391
25	Admin system	UBUNTU 20	ADMIN	FTP, MONGODB, SMTP, TOMCAT, TS 3, SSH	-
26	Admin system	UBUNTU 20	ADMIN	SSH, SNMP, POSTGRES, NTP	-
27	Admin system	UBUNTU 20	ADMIN	FTP, MONGODB, SMTP, TOMCAT, TS 3, SSH	CWE-1391
49-59	Compute node	UBUNTU 20	R&D	SPARK, HDFS	-
60	Compute node	DEBIAN WHEEZY	R&D	SPARK, HDFS, APACHE 2,SNMP, SSH	CVE-2014-6271
61	Compute node	DEBIAN 9.2	R&D	IRC, APACHE 2, SSH	CWE-89
62	Compute node	DEBIAN JESSIE	R&D	SPARK, HDFS, TS 3, TOMCAT, SSH	CVE-2010-0426
63	Compute node	DEBIAN JESSIE	R&D	SSH, SPARK, HDFS	CVE-2015-5602
64	Compute node	DEBIAN JESSIE	R&D	SAMBA, NTP, SSH, SPARK, HDFS	CVE-2017-7494

TABLE 6: Configuration of the target infrastructure shown in Fig. 1; vulnerabilities in specific software products are identified by the vulnerability identifiers in the Common Vulnerabilities and Exposures (CVE) database [53]; vulnerabilities that are not described in the CVE database are categorized according to the types of the vulnerabilities they exploit based on the Common Weakness Enumeration (CWE) list [54].

- [44] S. Banach, "Sur les opérations dans les ensembles abstraits et leur application aux équations intégrales," *Fundamenta Mathematicae*, 1922.
- [45] J. Hespanha and M. Prandini, "Nash equilibria in partial-information games on markov chains," in *Proceedings of the 40th IEEE Conference on Decision and Control (Cat. No.01CH37228)*, vol. 3, 2001.
- [46] K. Horák, B. Božanský, and M. Pěchouček, "Heuristic search value iteration for one-sided partially observable stochastic games," *Proceedings of the AAAI Conference on Artificial Intelligence*, Feb. 2017.
- [47] S. Bhattacharya, S. Badyal, T. Wheeler, S. Gil, and D. Bertsekas, "Reinforcement learning for pomdp: Partitioned rollout and policy iteration with application to autonomous sequential repair problems," *IEEE Robotics and Automation Letters*, vol. 5, no. 3, pp. 3967–3974, 2020.
- [48] S. Kullback and R. A. Leibler, "On information and sufficiency," *The Annals of Mathematical Statistics*, vol. 22, no. 1, pp. 79–86, 1951.
- [49] R. H. Berk, "Limiting Behavior of Posterior Distributions when the Model is Incorrect," *The Annals of Mathematical Statistics*, vol. 37, no. 1, pp. 51 – 58, 1966.
- [50] I. Esponda and D. Pouzo, "Equilibrium in misspecified Markov decision processes," *Theoretical Economics*, vol. 16, no. 2, pp. 717–757, 2021.
- [51] H. P. Reiser and R. Kapitza, "Hypervisor-based efficient proactive recovery," in *2007 26th IEEE International Symposium on Reliable Distributed Systems (SRDS 2007)*, 2007, pp. 83–92.
- [52] T. D. team, "Damn vulnerable web application (dvwa)," 2023, <https://github.com/digininja/DVWA>.
- [53] T. M. Corporation, "Cve database," 2022, <https://cve.mitre.org/>.
- [54] —, "Cwe list," 2023, <https://cwe.mitre.org/index.html>.
- [55] M. Kuhl, J. Wilson, and M. Johnson, "Estimation and simulation of nonhomogeneous poisson processes having multiple periodicities," in *Winter Simulation Conference Proceedings, 1995.*, 1995, pp. 374–383.
- [56] N. Nisan, T. Roughgarden, E. Tardos, and V. V. Vazirani, *Algorithmic Game Theory*. New York, NY, USA: Cambridge University Press, 2007.
- [57] D. Hernandez, K. Denamganai, Y. Gao, P. York, S. Devlin, S. Samothrakakis, and J. A. Walker, "A generalized framework for self-play training," in *2019 IEEE Conference on Games (CoG)*, 2019, pp. 1–8.
- [58] G. W. Brown, "Iterative solution of games by fictitious play," 1951, activity analysis of production and allocation.
- [59] J. Schulman, F. Wolski, P. Dhariwal, A. Radford, and O. Klimov, "Proximal policy optimization algorithms," *CoRR*, 2017, <http://arxiv.org/abs/1707.06347>.
- [60] J. Heinrich, "Reinforcement learning from self-play in imperfect-information games," Ph.D. dissertation, University College London, 2017.
- [61] T. Alpcan and T. Basar, *Network Security: A Decision and Game-Theoretic Approach*, 1st ed. USA: Cambridge University Press, 2010.
- [62] M. Tambe, *Security and Game Theory: Algorithms, Deployed Systems, Lessons Learned*, 1st ed. USA: Cambridge University Press, 2011.
- [63] T. Zhu, D. Ye, Z. Cheng, W. Zhou, and P. S. Yu, "Learning games for defending advanced persistent threats in cyber systems," *IEEE Transactions on Systems, Man, and Cybernetics: Systems*, 2022.
- [64] A. Aydeger, M. H. Manshaei, M. A. Rahman, and K. Akkaya, "Strategic defense against stealthy link flooding attacks: A signaling game approach," *IEEE Transactions on Network Science and Engineering*, vol. 8, no. 1, pp. 751–764, 2021.
- [65] O. Tsemogne, Y. Hayel, C. Kamhoua, and G. Deugoue, "Partially observable stochastic games for cyber deception against network epidemic," in *Decision and Game Theory for Security*, Q. Zhu, J. S. Baras, R. Poovendran, and J. Chen, Eds. Cham: Springer International Publishing, 2020, pp. 312–325.
- [66] E. Altman, K. Avrachenkov, and A. Garnae, "A jamming game in wireless networks with transmission cost," in *NET-COOP*, 2007.
- [67] K. C. Nguyen, T. Alpcan, and T. Basar, "Stochastic games for security in networks with interdependent nodes," in *2009 International Conference on Game Theory for Networks*, 2009, pp. 697–703.
- [68] Q. Zhu and T. Başar, "Dynamic policy-based ids configuration," in *Proceedings of the 48th IEEE Conference on Decision and Control (CDC) held jointly with 2009 28th Chinese Control Conference*, 2009.
- [69] H. Hu, Y. Liu, C. Chen, H. Zhang, and Y. Liu, "Optimal decision making approach for cyber security defense using evolutionary game," *IEEE Transactions on Network and Service Management*, vol. 17, no. 3, pp. 1683–1700, 2020.
- [70] S. A. Zonouz, H. Khurana, W. H. Sanders, and T. M. Yardley, "Rre: A game-theoretic intrusion response and recovery engine," in *2009 IEEE/IFIP International Conference on Dependable Systems & Networks*, 2009, pp. 439–448.
- [71] M.-F. Balcan, A. Blum, N. Haghtalab, and A. D. Procaccia, "Commitment without regrets: Online learning in stackelberg security games," in *Proceedings of the Sixteenth ACM Conference on Economics and Computation*, ser. EC '15. New York, NY, USA: Association for Computing Machinery, 2015, p. 61–78.
- [72] V. Lisy, T. Davis, and M. Bowling, "Counterfactual regret minimization in sequential security games," *Proceedings of the AAAI Conference on Artificial Intelligence*, vol. 30, no. 1, Feb. 2016.

- [73] L. Huang and Q. Zhu, "A dynamic games approach to proactive defense strategies against advanced persistent threats in cyber-physical systems," *Computers & Security*, vol. 89, p. 101660, 2020.
- [74] Z. Ni and S. Paul, "A multistage game in smart grid security: A reinforcement learning solution," *IEEE Transactions on Neural Networks and Learning Systems*, vol. 30, no. 9, pp. 2684–2695, 2019.
- [75] M. Yin, T. Li, H. Lei, Y. Hu, S. Rangan, and Q. Zhu, "Zero-shot wireless indoor navigation through physics-informed reinforcement learning," 2023, <https://arxiv.org/abs/2306.06766>.
- [76] E. J. Sondik, "The optimal control of partially observable markov processes over the infinite horizon: Discounted costs," *Operations Research*, vol. 26, no. 2, pp. 282–304, 1978.
- [77] R. Bellman, "A markovian decision process," *Journal of Mathematics and Mechanics*, vol. 6, no. 5, pp. 679–684, 1957.
- [78] M. L. Puterman, *Markov Decision Processes: Discrete Stochastic Dynamic Programming*, 1st ed. USA: Wiley, 1994.
- [79] D. Bertsekas, *Reinforcement learning and optimal control*. Athena Scientific, 2019.
- [80] R. B. Ash and C. Doléans-Dade, *Probability and Measure Theory*, ser. Academic Press. Academic Press, 2000.
- [81] C. T. Ionescu Tulcea, "Mesures dans les espaces produits," *Lincei-Rend. Sc. fis. mat. e nat.*, vol. 7, pp. 208–211, 1949.
- [82] D. Pollard, *A User's Guide to Measure Theoretic Probability*, ser. Cambridge Series in Statistical and Probabilistic Mathematics. Cambridge University Press, 2001.
- [83] P. Billingsley, *Convergence of probability measures*, 2nd ed., ser. Wiley Series in Probability and Statistics: Probability and Statistics. New York: John Wiley & Sons Inc., 1999, a Wiley-Interscience Publication.
- [84] C. D. Aliprantis and K. C. Border, *Infinite Dimensional Analysis: a Hitchhiker's Guide*. Berlin; London: Springer, 2006.